iScience

CellPress
OPEN ACCESS

Review

# Towards Truly Wearable Systems: Optimizing and Scaling Up Wearable Triboelectric Nanogenerators

K.R. Sanjaya D. Gunawardhana,[1] Nandula D. Wanasekara,[1] and R.D. Ishara G. Dharmasena[1,2,*]

## SUMMARY

**Triboelectric nanogenerator (TENG) is an upcoming technology to harvest energy from ambient movements. A major focus herein is harvesting energy from human movements through wearable TENGs, which are constructed by integrating nanogenerators into clothing or accessories. Textile-based TENGs, which include fiber, yarn, and fabric-based TENG structures, account for the majority of wearable TENGs, with many designs and applications demonstrated recently. This calls for a comprehensive analysis of textile-based TENG technology, and how the state-of-the-art device optimization concepts can be deployed to construct them efficiently. Concurrently, how advanced engineering concepts and industrial manufacturing techniques, which are bound with fiber, yarn, and fabric-related developments, can be applied into the TENG context for their output enhancement is still under investigation. Herein, we fill this vital gap by analyzing the state-of-the-art developments, upcoming trends, output optimization strategies, scalability, and prospects of the textile-based TENG technology, presenting a textile engineering perspective.**

## INTRODUCTION

Upcoming technologies such as the Internet of Things (IoT) and 5G technology are reshaping the future role of textiles and apparels (Dharmasena and Silva, 2019a, 2019b). The next generation of smart textiles will have advanced capabilities of interacting with the user and the environment, creating a broad range of applications in communication, health care, security, sports, education, and consumer electronics (Dharmasena et al., 2019; Dharmasena and Silva, 2019a, 2019b; Fernando et al., 2017; Wijesena et al., 2016; Stoppa and Chiolerio, 2014; Wang et al., 2015a, 2015b, 2015c, 2015d; Weng et al., 2016; Yetisen et al., 2016). In recent examples, smart textiles have been used in real time to monitor body motion and muscle behavior and to diagnose physiological parameters such as temperature, blood pressure, heart rate, etc., with the detected signals incorporated into electrocardiogram, electroencephalogram, and electromyogram and observed via IoT and smart electronic devices (Ahn et al., 2015; Koo et al., 2014; Manero et al., 2016; Stoppa and Chiolerio, 2014).

The electronic components integrated within smart textiles and wearable electronics consume varying degrees of power, ranging from microwatts to milliwatts (Figure 1A). Finding methods to power these devices while maintaining their wearable and electronic performances is challenging (Dharmasena et al., 2019; Dharmasena and Silva, 2019a, 2019b; Paosangthong et al., 2019a; Wu et al., 2019). Conventionally, wired power supplies and rechargeable or replaceable energy storage units were used for this purpose; however, with increasing performance requirements, these are becoming obsolete. Energy harvesting, which captures freely available energy from the ambient environment and converts into electricity, has emerged as a potential candidate to replace, or combine with, the existing energy technologies (Figure 1B) (Dharmasena et al., 2019; Tian et al., 2017; Wang et al., 2015a, 2015b, 2015c, 2015d). Among available energy sources, human motion generates considerable mechanical power (Figure 1C) and is closely related to wearable technologies, drawing significant attention worldwide as a viable energy source for wearable electronics (Figure 1C) (Dharmasena and Silva, 2019a, 2019b).

Triboelectric nanogenerators (TENGs) have emerged at the forefront of harvesting human motion to power wearable technologies, due to their many unique features such as high outputs and efficiency, flexibility, durability, ease of fabrication, and low cost. First reported by Z. L. Wang's research group in 2012 (Fan et al., 2012) TENG research has experienced a rapid expansion in recent years (Ding et al., 2019). TENGs

[1]Department of Textile and Clothing Technology, Faculty of Engineering, University of Moratuwa, Bandaranayake Mawatha, Moratuwa 10400, Sri Lanka

[2]Wolfson School of Mechanical Electrical and Manufacturing Engineering, Loughborough University, Loughborough, Leicestershire LE11 3TU, UK

*Correspondence: r.i.dharmasena@lboro.ac.uk

https://doi.org/10.1016/j.isci.2020.101360

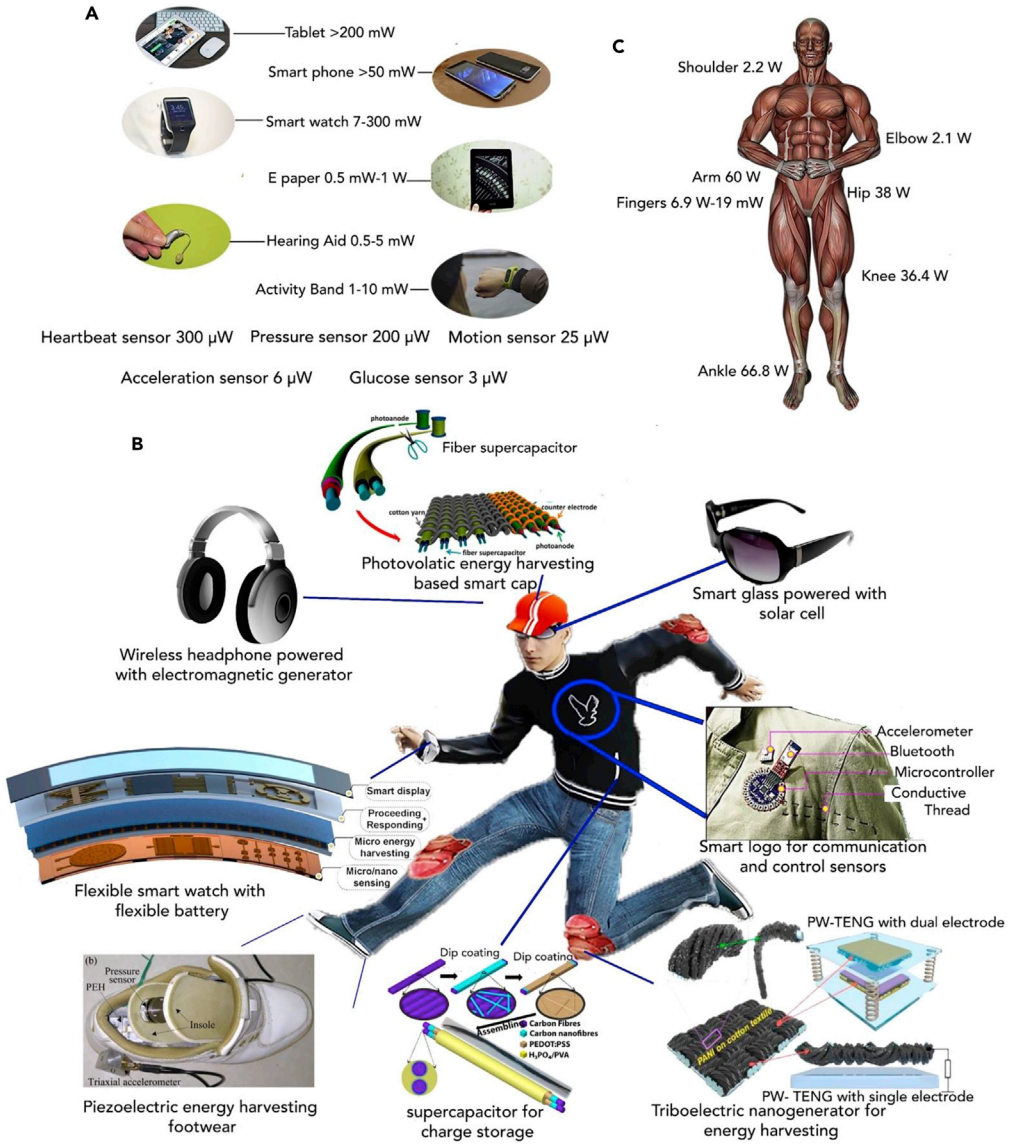


**Figure 1. Energy Harvesting for Wearable Electronics**

(A) Power requirements of various portable electronics. Adopted from ref (Byun et al., 2017) (B) Schematic of energy sources for wearable devices. (Flexible smart device reprinted from ref (Zhang et al., 2018) with permission, Copyright©2018 Elsevier Ltd. Triboelectric nanogenerator reprinted from ref (Dudem et al., 2019) with permission, Copyright©2018 Elsevier Ltd. Supercapacitor for charging reprinted from ref (Dong et al., 2017b) with permission, Copyright©2017 American Chemical Society. Photovoltaic energy harvesting reprinted from ref (Chai et al., 2016) with permission, Copyright©2016 American Chemical Society. Piezoelectric energy harvesting shoe reprinted from ref (Fan et al., 2017) with permission, Copyright©2017 AIP Publishing. Smart logo for communication and control sensors reprinted from ref (Jung et al., 2015) with permission, Copyright©2015 Springer Nature.) (C) Average energy generation in different regions of the body during mild physical activities (walking movement of an average person). Adopted from (Dharmasena and Silva, 2019a, 2019b; Invernizzi et al., 2016; Riemer and Shapiro, 2011).

are especially useful in textile-based energy harvesting applications, as they can be readily designed and integrated into clothing. Many of the conventional textile materials listed in the triboelectric series (Dong et al., 2018; Guo et al., 2018; Pu et al., 2015; Zhou et al., 2014a, 2014b) have been demonstrated to produce wearable TENGs with desirable output performances and wearable characteristics. In addition, TENGs have been integrated into textiles using common manufacturing techniques such as weaving, knitting,

braiding, embroidery, etc. (Chen et al., 2018; Dharmasena and Silva, 2019a, 2019b; Dong et al., 2017b). To this end, the properties of textile materials, textile structures, and processing techniques play a pivotal role in influencing wearable TENG performances.

Despite many device examples, only a limited number of reports exist that help to systematically understand the behavior of textile-based TENGs and their optimization strategies. The relationship between the fiber, yarn, fabric, and garment behavior; their production techniques; and how these affect the electrical and mechanical performance of wearable TENGs are yet to be studied. Such investigations would be critical because the successful development of wearable energy generation units and their mass-scale production depend on the detailed understanding of the interrelationship between the textiles and the electronic components.

Herein, we conduct a detailed investigation of the available literature for textile-based TENGs, with regard to the various stages of the textile manufacturing process. First, we provide a generic introduction to TENG basics including their types, working principles, and optimization methods. Next, a brief overview of the textile manufacturing process and textile-based wearable TENGs is provided. For the first time, we present the categorization of textile-based TENGs according to different stages of the textile manufacturing process. Within this classification, key features of current textile-based TENGs, potential optimization strategies, and scalability are discussed in detail, providing a textile engineering perspective on how to overcome major challenges in this research area. A series of guidelines are provided for fiber, yarn, and fabric-based TENGs to make them compatible with the established textile techniques and processes. Finally, the measurement techniques, standardization strategies, and prospects of the textile-based TENGs are examined, paving the way toward sustainable future wearable applications.

## FROM TENG BASICS

A number of fundamental working modes were introduced for TENGs, depending on their structure and motion profile, namely, vertical contact separation mode, lateral sliding mode, single-electrode mode (SE-TENG), and free-standing triboelectric layer mode (FSTENG) (Figure 2A) (Wang et al., 2015a, 2015b, 2015c, 2015d). The working principles of all the TENG categories rely on two fundamental phenomena: triboelectric charging and electrostatic induction.

### Triboelectric Charging and Material Selection

Triboelectric charging is the static charge separation between two material surfaces when contacted with each other (Baytekin et al., 2011a; Dharmasena and Silva, 2019a, 2019b; Galembeck et al., 2014). The origin of triboelectric charging is assumed to be due to electron (Liu and Bard, 2008; Xu et al., 2018), ion (McCarty and Whitesides, 2008), or charged material transfer (Baytekin et al., 2012, 2011b), or several of these charge types (Galembeck et al., 2014). The ability of a surface to be triboelectrically charged with respect to a reference surface is empirically utilized to construct the triboelectric series (Diaz and Felix-Navarro, 2004; Zou et al., 2019). Incidentally, triboelectric series contains a large number of common textile polymers and materials (Figure 2B) (Liu et al., 2018a, 2018b), which facilities the use of existing textile materials for TENG applications (Zou et al., 2019). For instance, textile substrates composed of dielectric polymers such as cotton (Chen et al., 2018; Ning et al., 2018), silk (Choi et al., 2017; He et al., 2020; Ye et al., 2020a), nylon (Gong et al., 2017), polyester (Dong et al., 2017a; Pu et al., 2016a), polyethylene terephthalate (PET) (Xiong et al., 2018; Zhang et al., 2016), polylactic acid (Pan et al., 2018), polyurethane (PU) (Kim et al., 2019), and carbon fibers (Chen et al., 2018) have been used as wearable TENG contact surfaces. In some cases, additional triboelectric coatings using materials such as polytetrafluoroethylene (PTFE) (Cheng et al., 2017; Ning et al., 2018), polydimethylsiloxane (PDMS) (Dong et al., 2017a; Lee et al., 2015), silicone rubber (Pan et al., 2018), perylene (Zhang et al., 2016), and polyvinylidene fluoride (PVDF) (Guo et al., 2018), which are also associated with textiles, were used to enhance triboelectric performance. On the other hand, TENG electrodes and conductive interfaces have been constructed using metals and metal nanoparticles (Lee et al., 2015; Seung et al., 2015), carbon-based materials such as carbon nanotubes (CNTs) (He et al., 2017), and conductive polymers such as polyaniline (Dudem et al., 2019), in the form of embedded wires or surface coatings.

Material selection for triboelectric contact surfaces is critical, as it primarily affects triboelectric charging. We previously demonstrated the effect of triboelectric charging on the output optimization of TENGs, where the power output increased quadratically against increasing triboelectric charge density

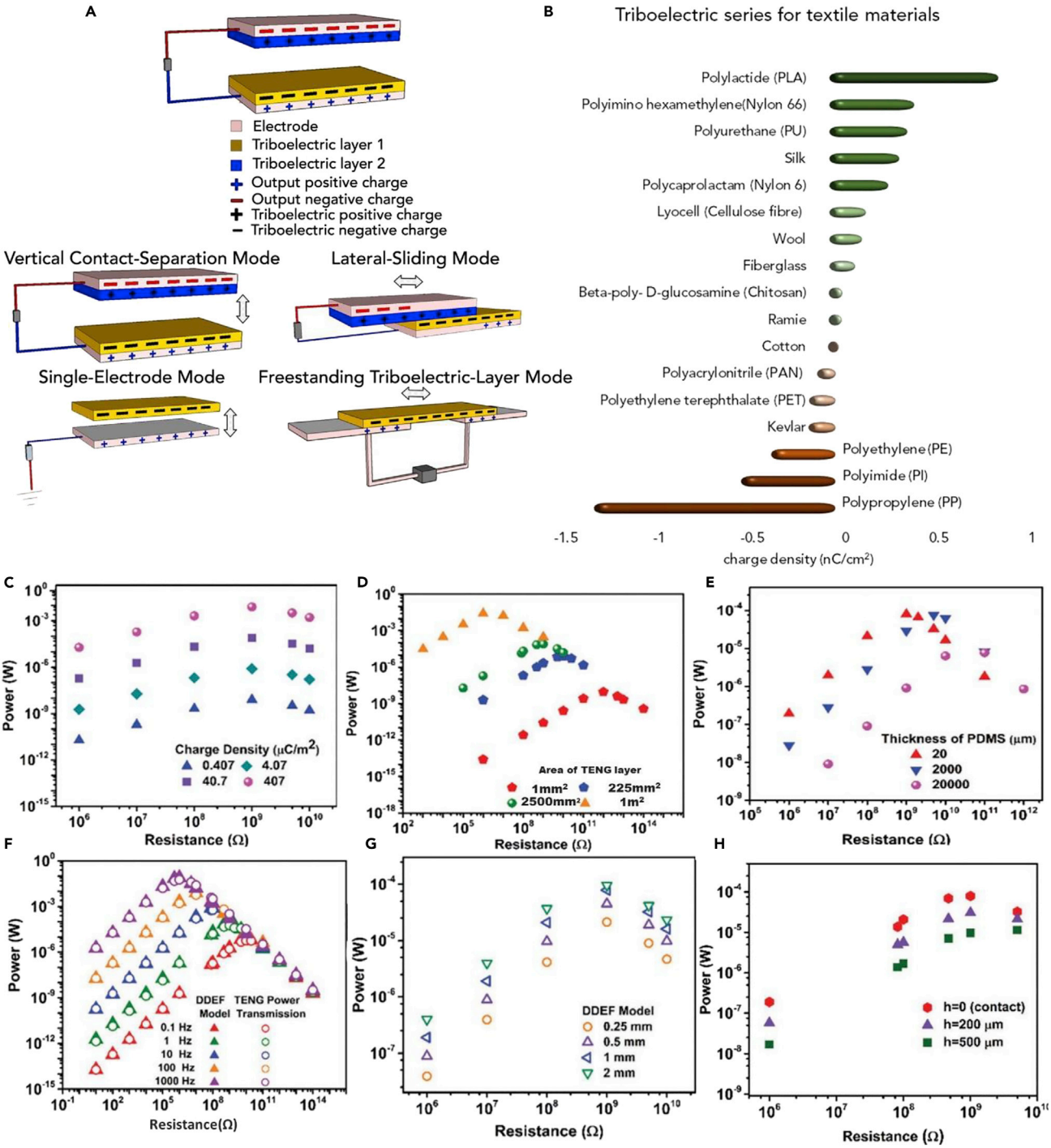


**Figure 2. Types of TENGs and Their Design Parameters**

(A) Schematic of basic TENG working modes. Adopted from (Dharmasena and Silva, 2019a, 2019b).

(B–E) (B) Several common textile materials included in the triboelectric series. Adopted from (Liu et al., 2018a, 2018b). DDEF model simulations for the effect of (C) increasing triboelectric charge density, (D) increasing triboelectric surface area, and (E) increasing triboelectric layer thickness on TENG output power density.

(F–H) (F) DDEF model and TENG power transfer theory simulations for the effect of increasing rate of movement (frequency) of TENG layers on its output power density. The DDEF model simulations for the effect of (G) increasing amplitude of the movement and (H) minimum separation between TENG contact surfaces (contact or non-contact motion regime), on TENG output power density. Reprinted from (Dharmasena et al., 2018a, 2018b) with permission, Copyright© 2018 The Authors.

(Dharmasena et al., 2018a, 2018b), whereas the optimum resistance (i.e., the external load that extracts the maximum power from the TENG) remained constant (Figure 2C). Selecting material types further apart in the triboelectric series, providing sufficient contact between triboelectric surfaces, and enhancing triboelectric contact area by increasing surface roughness are some of the commonly used techniques for triboelectric charge density enhancement, which are applicable for optimizing textile-based TENGs (Dharmasena et al., 2018a, 2018b; Dharmasena and Silva, 2019a, 2019b). On the other hand, selecting high conductivity materials for TENG electrodes is essential to keep the device impedance low, efficiently induce device outputs, and to effectively extract output power. In terms of wearable TENG applications, the material selection process should target to achieve a balance between electrical performances and wearable characteristics.

## Electrostatic Induction and Output Enhancement

The relative movement of triboelectrically charged surfaces induces an output on the TENG electrodes (Deane et al., 2018; Dharmasena et al., 2017; Dharmasena et al., 2018a, 2018b; Dharmasena and Silva, 2019a, 2019b). This behavior is governed by the variation of the electric fields acting on the electrode interfaces of TENG units, resulting in the generation of Maxwell's displacement current, as described by Wang (2017),

$$J_D = \frac{\partial D}{\partial t} = \varepsilon \frac{\partial E}{\partial t} + \frac{\partial P_S}{\partial t} \quad \text{(Equation 1)}$$

where $J_D$ is displacement current density, $D$ is displacement field, $t$ is time, $E$ is the electric field, $\varepsilon$ is the permittivity, and $P_S$ is the polarization of the medium.

The output behavior of TENG was initially explained using a capacitor-based circuit model, by developing a relationship between voltage ($V$), charge ($Q$), and TENG layer separation ($x$) (known as the V-Q-x relationship) given by (Niu et al., 2013)

$$V = -\frac{1}{C(x)} Q + V_{OC}(x) \quad \text{(Equation 2)}$$

where $V_{OC}(x)$ represents the open-circuit voltage and $c(x)$ represents the capacity. This model contained several drawbacks including the difficulty in fully explaining TENG working principles and closely approximating output trends of practical TENG devices. Consequently, we presented the distance-dependent electric field (DDEF) model based on Maxwell's equations, to fully describe the working principles of TENGs (Dharmasena et al., 2017; 2018a, 2018b). This model accounts for the finite dimensions of triboelectrically charged sheets to predict their electric field behavior. For instance, the fundamental electric field equation for the DDEF model approximates the electric field of a charged sheet with length (L), width (W), charge density ($\sigma$), and dielectric constant ($\varepsilon$), against distance $z$ using (Dharmasena et al., 2017)

$$E_Z = \frac{\sigma}{\pi\varepsilon} \arctan\left( \frac{L/W}{2(Z/W)\sqrt{4(Z/W)^2 + (L/W)^2 + 1}} \right) = \frac{\sigma}{\pi\varepsilon} f(z) \quad \text{(Equation 3)}$$

Considering the electric fields of the triboelectrically charged layers and output charge layers, the overall electric field at the electrode interfaces can be calculated, which is used to evaluate the potential of the electrodes (Dharmasena et al., 2017). Consequently, the voltage, current, charge, and power outputs of the TENG can be predicted using the DDEF model with a relatively higher accuracy (Dharmasena, 2019; Dharmasena et al., 2017; 2018a, 2018b).

Based on the DDEF model, we presented optimization criteria to significantly enhance the structural, material, and motion parameters of a TENG, which can act as a guideline to improve textile-based TENG performances. Considering structural parameters, larger triboelectric contact surface areas are favorable for higher power generation and to reduce TENG internal impedance (Figure 2D). Lower thicknesses of triboelectric layers provide favorable output trends, given that the thickness is sufficient for the stable accumulation of triboelectric charges (Figure 2E). Textiles are available in a variety of thicknesses (microns to millimeters) and sizes (up to several square meters for clothing), and therefore can be engineered to fit the energy harvesting applications. In terms of material parameters, the dielectric constant is again a key material parameter affecting TENG performances. As evident from Figure 2B a large number of textile materials are available for TENGs, enabling both charge density improvement and engineering of the dielectric

constant. With regard to motion parameters, faster relative movements (Figure 2F) (Dharmasena et al., 2018a, 2018b) and higher motion amplitudes (Figure 2G) ensuring adequate contact between triboelectric surfaces (Figure 2H) are critical in improving the power output of a TENG. Therefore, textile techniques that introduce elasticity, flexibility, and rapid movement to textile structures via material selection and fabric structuring (that will be discussed in future sections of this work) are extremely beneficial in constructing highly efficient TENG designs.

## TEXTILE-BASED TENGS

### Overview of the Textile Manufacturing Process

The starting point of textile products is "fiber." Fibers are distinguished by their high length to diameter ratio (McIntyre and Daniels, 1995), which is typically over several hundred times for textile fibers. Natural fibers used for textiles include plant-based seed fibers (e.g., cotton, kapok), bast fibers (e.g., flax, jute, hemp), leaf fibers (e.g., abaca, manila), and animal-based fibers (e.g., wool, silk, alpaca) (Eichhorn et al., 2009; Todor et al., 2018). Prominent man-made fibers include synthetic fibers such as polyamide (PA); PET; polyvinyl alcohol (PVA); polypropylene; polyvinyl chloride; polyethylene; regenerated cellulose fibers such as lyocell, viscose, and modal; and other high-performance fibers (Foster et al., 2018; Wanasekara et al., 2016, 2012; Wanasekara and Eichhorn, 2017; Zhu et al., 2016a, 2016b). Depending on their length, fibers are divided into staple fibers (short in length) and filaments (continuous fiber strands). Common textile manufacturing process follows the steps of fibers (Figure 3A), yarns (Figures 3B–3D), fabrics (Figures 3E–3I), and garments (Figures 3M–3Q).

Conversion of fibers into yarns is realized through spinning or extrusion. Spinning is predominantly used for the conversion of staple fibers into yarns. Considering the example of a natural fiber (cotton), several substages are involved in this process known as ginning (removing fibers from seed), bailing (Figure 3C (1)), opening (Figure 3C (2)), carding (Figure 3C (3)) (opening into individual fibers) (Lee and Ockendon, 2006), drawing (Figure 3C (4 and 5)) (orientation of the fibers), and twisting (Figure 3C (6)) (to increase fiber cohesion) (Lawrence, 2010). Ring spinning technique used in this example enables strong fiber binding via a uniform twist and produces hairy yarns with fiber protrusions, which could be important to increase yarn surface area. There are other techniques such as rotor, air jet, friction, and wrap spinning, providing various degrees of strength, uniformness, and extensibility (Lawrence, 2010). Yarn parameters such as composition, count, twist, production mechanism, and lifespan would influence the mechanical and electrical performance of wearable TENGs.

Filament fibers can be directly converted into yarns using different extrusion techniques (Lawrence, 2010). Common extrusion techniques include wet spinning (polymer dissolved in a solvent and extruded from spinneret submerged in a chemical bath), dry spinning (polymer dissolved in a solvent that is evaporated with hot air after extrusion), melt spinning (George, 1982) (Figure 3B) (polymer melted before extruding), and gel spinning (polymer is in gel form, which passes through the air, followed by a liquid bath) (McIntyre, 2005).

Common methods of manufacturing fabrics from yarns include nonwoven (Figure 3E), weaving (De Pauw et al., 2020) (Figure 3F), and knitting (Figure 3G), after which the fabrics are subjected to dyeing (Figures 3H–3K), finishing (Figure 3L), and garment manufacturing processes (Figures 3M and 3N), along with additional operations such as printing (Figures 3O and 3P) and embroidery (Figure 3Q) for special requirements.

Woven fabrics are formed by interlacing two sets of yarns known as warps (lengthwise) and wefts (widthwise) in a right angle. Some of the weaving designs include plain weave (Figure 4A), twill (Figure 4B), sateen (Figure 4C), and satin (Figure 4D) (Adanur, 2000). The manufacturing techniques for weaving include single-phase and multi-phase methods. Single-phase weaving includes shuttle weaving and shuttle-less weaving methods (e.g., air jet, water jet, rapier, and projectile). In the multi-phase category, circular and flat weaving techniques are prominent. Advanced weaving methods such as 3-dimensional (3D) weaving have become increasingly popular, adding structural functionalities to textiles (Harvey et al., 2019; Schegner et al., 2019), which could be useful in developing custom-made high-performance TENGs.

Knitted fabrics are manufactured by interlooping yarns using weft knitting (Figure 4E) or warp knitting (Figure 4F). Weft knitting uses yarns to produce the loops in the horizontal direction (width direction) of the fabric (courses). Some of the common weft-knitted fabric structures include plain (Figure 4G), rib

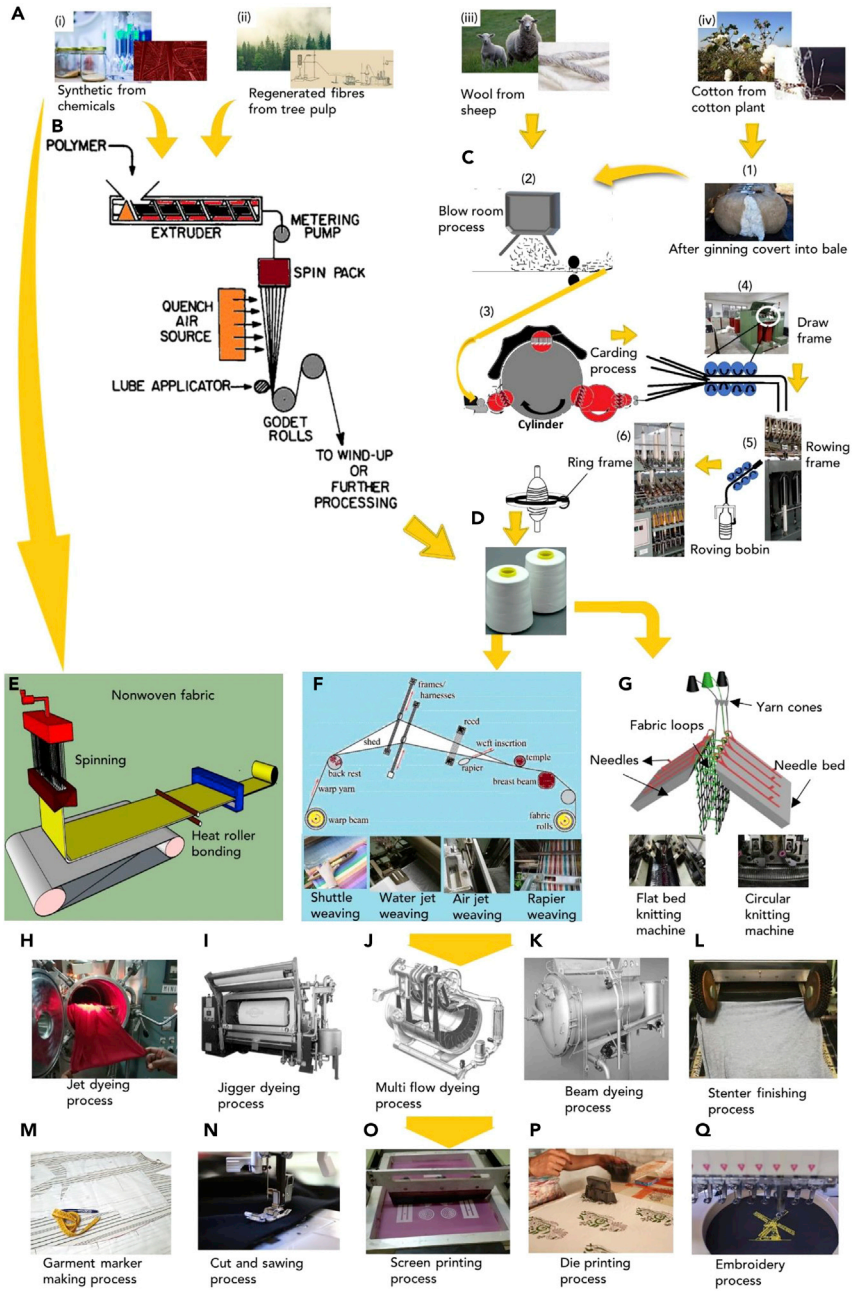


**Figure 3. Textile Manufacturing Process Depicting Fiber, Yarn, Fabric, and Garment Stages**

(A) Fiber stage showing (i) synthetic fibers, (ii) regenerated fibers, (iii) wool fibers, and (iv) cotton fibers.

(B) Synthetic yarn manufacturing process (melt spinning). Reprinted from ref (George, 1982), with permission, Copyright©1982 Society of Plastics Engineers Inc.

(C) Cotton yarn manufacturing process: (1) bale preparation, (2) blow room operation, and (3) carding operation. Reprinted from ref (Lee and Ockendon, 2006), with permission, Copyright©2006 Springer Nature. (4) Draw frame operation, (5) roving frame operation, and (6) ring frame operation.

(D) Final yarn packaging.

(E) Non-woven fabric manufacturing (polymer laid method).

(F) Schematic of weaving. Reprinted from ref (De Pauw et al., 2020), with permission, Copyright©2019 SAGE Publications (weaving operations: shuttle, air jet, water jet, rapier).

(G–K) (G) Schematic of knitted fabric manufacturing. Reprinted from ref (Zhu et al., 2016a, 2016b), with permission, Copyright©2016 Elsevier Ltd. (knitting operations: flatbed, circular). Dyeing and finishing operations, depicting (H) jet

**Figure 3. *Continued***
dyeing (I) jigger dyeing (J) multiflow dyeing (K) beam dyeing (I, J, and K reprinted from ref (Nair, 2011), with permission, Copyright©2011 Elsevier).
(L–Q) (L) Stenter process for fabric finishing. Garment manufacturing process, showing (M) marker making, (N) cut and sawing, (O) screen printing, (P) die printing, and (Q) embroidery processes.

(Figure 4H), interlock (Figure 4I), and purl (Figure 4J). Specialty knitted fabrics such as 3D knitted and spacer fabrics (Zhu et al., 2016a, 2016b) are interesting prospects for textile TENGs due to their desired structural and mechanical functionalities.

In warp knitting, a set of yarns is used to construct loops in the vertical direction (length direction) of the fabric (wales) (Spencer, 2001). Tricot and Raschel are the two main types of warp knit fabric structures. Knitted fabrics allow more design capabilities, along with properties such as stretchability, and conformity, demonstrating the potential to be popular in next-generation smart textile applications (Kwak et al., 2017). A performance comparison between woven and knitted fabrics, which are critical for most of the TENG developments, is provided in Note S1.

Nonwoven process directly converts fibers into fabrics through mechanical or chemical processes, bypassing yarn manufacturing. Nonwoven fabrics have found a variety of applications, especially as technical textiles. These fabrics are produced using techniques such as dry-laid (fibers bonded by mechanical, thermal or chemical processes), wet-laid (similar to paper production), and polymer laid (Figure 3D) (synthetic filaments extruded by molten polymer) (Russell, 2007) methods, and their physical properties vary according to the production method.

Once a fabric is produced, it is subjected to finishing operations. This includes major steps such as coloration of the fabrics via techniques such as dyeing and printing (Wardman, 2017). The type of colorants and the coloration processes vary significantly depending on the fiber type as summarized in Note S2. Following textile production, internationally recognized standards are used to evaluate their quality.

## Overview of Textile-Based Wearable TENGs

A large variety of wearable TENG designs have been reported in the literature using flexible polymer-based and textile-based architectures. In this article, we focus on textile-based TENG developments. Note S3 summarizes some of the significant textile-based TENG developments, based on common textile materials.

From a textile engineering perspective, these TENGs can be linked to different stages of the textile manufacturing process summarized in Figure 3. Therefore, in the upcoming sections of this work (sections Fiber/Yarn-Related TENG Developments and Fabric-Related TENG Developments), we categorize the textile-based TENGs into fiber/yarn-related developments (relevant to processes depicted in Figures 3A–3D), and fabric-related developments (relevant to processes depicted in Figures 3E–3Q), to analyze their performance, optimization procedures, scaling up, and potential performance improvement methods. The main parameter that we use for this classification is the stage at which the textile material is triboelectrically functionalized, providing a logical basis for the categorization of textile-based TENGs.

However, it is important to note that the TENG technology is still in its early stages; therefore almost all the fabrication methods are laboratory-based processes that are comparable with the manufacturing techniques described in Figure 3. Typically, such fabrications take place in the form of triboelectric modifications in yarn or fabric form. For instance, the fiber/yarn-based TENG fabrication methods include laboratory-scale electrospinning (Li et al., 2020), wrapping or coiling with a motor (Lou et al., 2020; Ye et al., 2020a), twisting techniques (Zhou et al., 2014a, 2014b), etc. These yarns and fibers are typically embedded or converted into fabrics using sewing (He et al., 2019; Lai et al., 2017), hand weaving (Liu et al., 2019a, 2019b; Zhang et al., 2016), shuttle weaving (Chen et al., 2016), hand knitting (Dong et al., 2017b), pilot-scale nonwoven techniques (Peng et al., 2019), and embroidery (Sala de Medeiros et al., 2019) methods. On the other hand, fabric-based TENG developments utilize techniques such as dip coating and dyeing (Chen et al., 2018; Ko et al., 2015; Pu et al., 2015; Seung et al., 2015), spin coating (Lee et al., 2015), plasma treatment (Matsunaga et al., 2020), screen printing (Paosangthong et al., 2019b), electrodeposition (Zhu et al.,

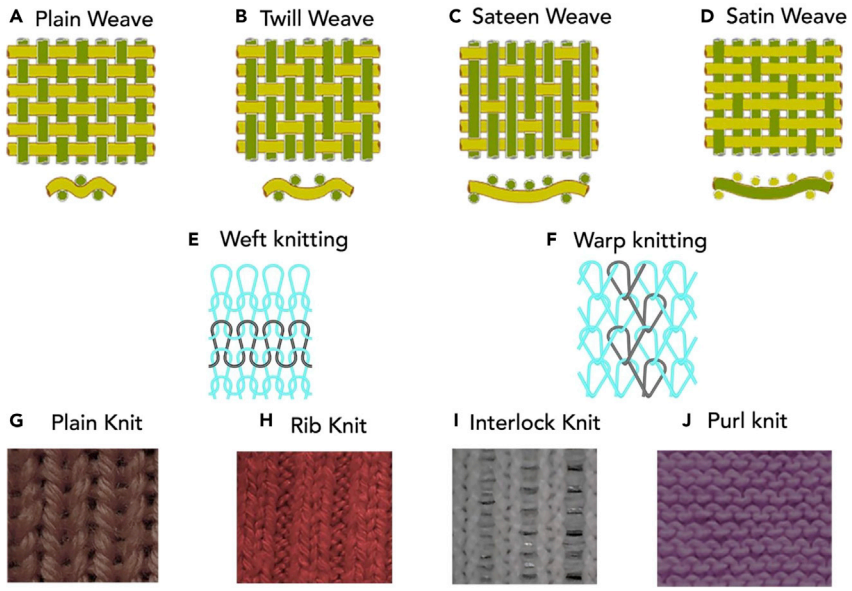


**Figure 4. Schematics of Basic Woven and Knitted Fabric Structures**

(A–J) Weave patterns depicting (A) plain weave, (B) twill weave, (C) sateen weave, and (D) satin weave. Adopted from ref (Adanur, 2000). A generic schematic representation of (E) a weft-knitted and (F) a warp-knitted fabric. Photographs of weft-knitted designs, depicting (G) plain knit, (H) rib knit, (I) interlock knit, and (J) purl knit. Adopted from ref (Spencer, 2001).

2012), reactive ion etching (Ye et al., 2020b), lithography (Zhang et al., 2019), etc., to triboelectrically modify the contact surface or fabric structure. With this review, we also develop a link between the laboratory- and the industry-based processes explained in Figure 3, through a detailed discussion on optimization and scaling up of textile-based TENG technology (sections Future Perspectives of Fiber/Yarn-Based TENG and Future Perspectives for Fabric-Based TENG Devices).

## FIBER/YARN-RELATED TENG DEVELOPMENTS

In our classification, fiber- and yarn-based TENGs include the TENG designs in which the major triboelectrically active modifications correspond to one of the stages depicted in Figures 3A–3D of the textile manufacturing process. Considering their structure, fiber/yarn-related TENGs are divided into two sub-categories: core-shell and sandwiched structures. TENG developments at fiber/yarn stage allow for maximum control and modification capabilities of the energy generators (Liu et al., 2019a, 2019b; Ma et al., 2020; Ye et al., 2020a; Yu et al., 2017); however, their handling and processing have been difficult due to small size and weak mechanical properties.

### Core-Shell Fiber/Yarn-Based TENGs

Core-shell fiber and yarn structures are popular for energy harvesting and self-powered sensing. Some of the core-shell TENGs operate in single-electrode mode in which the human skin acts as the counter-triboelectric surface (Dong et al., 2018, 2017b; Park et al., 2017), whereas some reports indicate duel core-shell structures that contain two triboelectric layers and two electrodes (Liu et al., 2019a, 2019b; Tian et al., 2018; Ye et al., 2020b, 2020a). Core-shell structure allows the core material to be protected within the surrounding sheath structure (Cheng et al., 2017; He et al., 2017), with additional advantages such as ease of fabrication and ability to withstand mechanical stresses.

Considering device examples for energy harvesting, Ye et al. (2020a) developed an energy harvesting textile by wrapping silk and PTFE fibers (triboelectric surfaces) around stainless-steel core yarns (electrodes) (Figure 5A). Shuttle loom weaving and embroidery techniques were used to construct a fabric using these functional yarns, producing a peak $V_{OC}$~45 V, peak $J_{SC}$~ 0.2 mA/m$^2$, and peak power density of 3.5 mW/m$^2$ through a load of 50 MΩ, under a contact separation movement at 2 Hz.

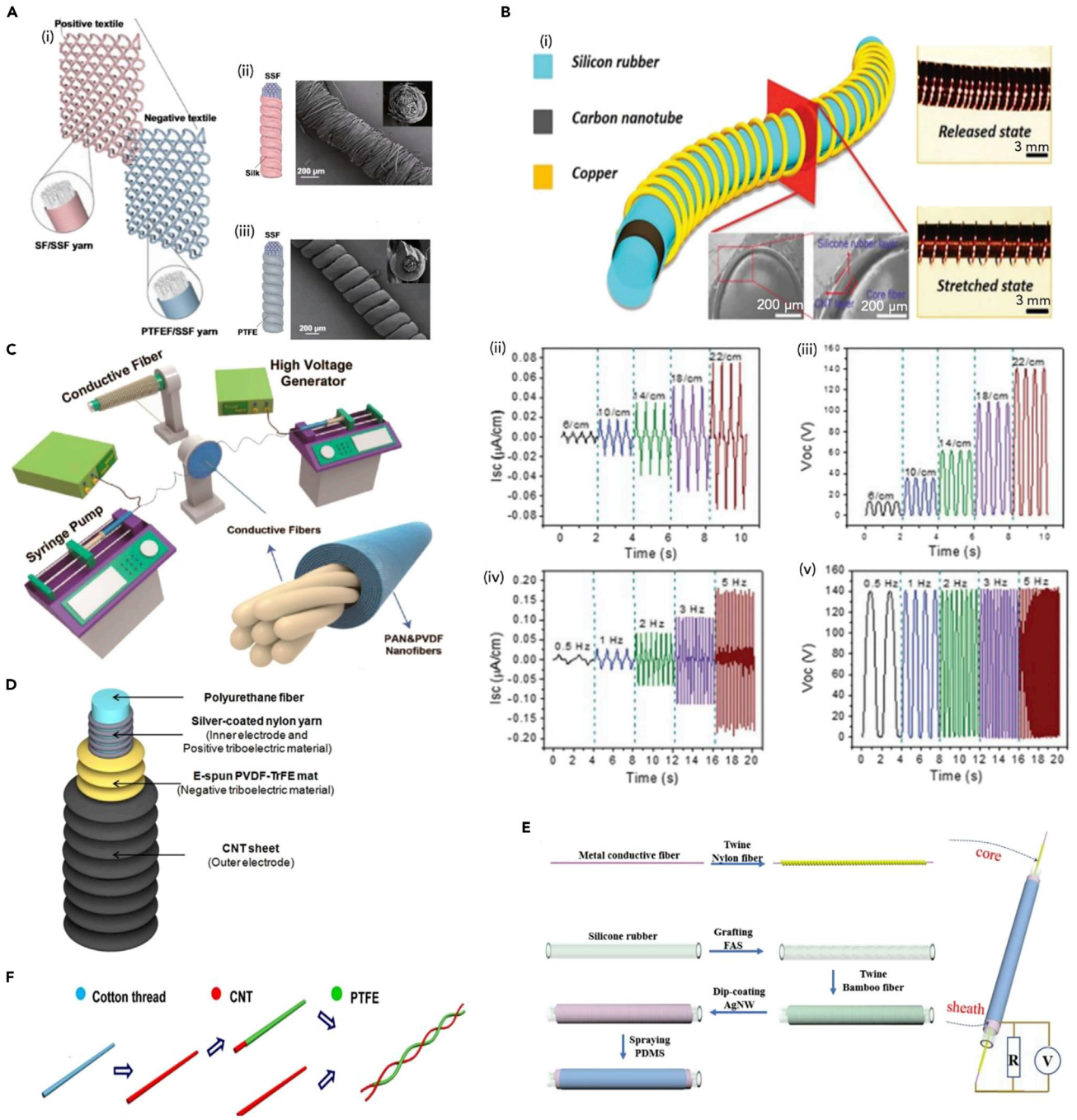


**Figure 5. Core-Shell Fiber/Yarn Based TENG Developments**

(A) Schematic of silk/stainless-steel fiber (SF/SSF) and PTFE/stainless-steel fiber (PTFE/SSF)-based TENG. Corresponding SEM images for (ii) SF/SSF and (iii) PTFE/SSF. Reprinted from ref (Ye et al., 2020a) with permission, Copyright©2019 Springer Nature.

(B) (i) Schematic of a TENG based on a coiled electrode, consisting of silicone rubber, CNT, and copper. Variation of outputs against increasing number of coils per cm (at 50% strain and 2 Hz frequency) demonstrating (ii) $I_{SC}$ and (iii) $V_{OC}$ and variation of outputs against increasing frequency of movement (22 coils/cm, 50% strain) demonstrating (iv) $I_{SC}$ and (v) $V_{OC}$. Reprinted from ref (He et al., 2017) with permission, copyright©2016 WILEY-VCH Verlag GmbH & Co.

(C) Development of a SETENG with silver yarn as the core and PVDF and PAN hybrid nanofibers as the shell, using electrospinning. Reprinted from ref (Ma et al., 2020) with permission, Copyright©2020 American Chemical Society.

(D) Schematic of silver-coated nylon yarn-wrapped PU fiber TENG. Reprinted from ref (Sim et al., 2016) with permission, Copyright©2016 Springer Nature.

**Figure 5. *Continued***

(E) Schematic of the fabrication process of wavy-structured covering yarn-based TENG. Reprinted from ref (Gong et al., 2017) with permission, Copyright©2017 Elsevier.

(F) Schematic of the fabrication process of the twisted fiber-based TENG constructed using cotton yarns with CNT and PTFE. Reprinted from ref (Zhou et al., 2014a, 2014b) with permission, Copyright©2014 American Chemical Society.

He et al. (2017). constructed a multi-layered stretchable and flexible fiber-like TENG (Figure 5B). A silicone rubber fiber was coated with a CNT-based conductive composite ink that acted as an electrode. This was covered by another silicone layer. A copper microwire was wrapped around the outer silicone layer, which acted as the second electrode. Triboelectric charging, in this case, took place between the copper wire and the silicone rubber surface. When relaxed, the copper electrode and the silicone layer are in contact; however, when the fiber is stretched, a gap is created between these two surfaces. This creates a contact and separation action during the stretch and recovery of the fiber, and correspondingly, a current is driven between the copper wire and the CNT electrode. When subjected to 50% stretch (number of coils 22 $cm^{-1}$ and 5 Hz frequency, 10 cm length), the device produced peak performances of $V_{OC}$~140 V, $I_{SC}$ ~ 0.18 μA/cm, and charge density 6.1 nC/cm. Peak power of 5.5 μW was obtained through a 320 MΩ load, when the fiber was subjected to 50% stretch at 2 Hz frequency. The applicability of the TENG in energy harvesting was demonstrated by powering a digital watch and a calculator.

Core-shell TENG fibers have also been demonstrated in a number of self-powered sensing applications (Ha et al., 2015; He et al., 2019; Wang et al., 2015a, 2015b, 2015c, 2015d). Ma et al. developed a triboelectric yarn using a silver yarn as the core. The shell was fabricated with PVDF/polyacrylonitrile (PAN) hybrid nanofibers via electrospinning (Figure 5C) (Ma et al., 2020). The triboelectric yarn indicated low weight (0.33 mg/cm), softness, and low diameter (350.66 μm). This yarn was processed into a TENG fabric using weaving and operated in SETENG mode, generating a voltage of 40.8 V, current of 0.705 μA/cm, and charge density of 9.513 $nC/cm^2$ under a movement of 2.5 Hz and 5 N force. Furthermore, a power output of 336.2 μW/m was generated at 1 Hz operating frequency. A load sensor was constructed using the triboelectric yarn by developing a woven 8 × 8-pixel array, capable of detecting the pressure, location, and magnitude of the applied load.

In another sensing example, Sim et al. developed a stretchable multi-layered core-shell and wrinkled TENG fiber (Figure 5D) (Sim et al., 2016). Herein, a silver-coated nylon yarn wrapped around a PU fiber acted as an electrode and positive triboelectric layer. An electrospun polyvinylidene fluoride-co-trifluoroethylene (PVDF-TrFE) mat was wrapped around this fiber, which acted as the native triboelectric material, whereas the outer electrode consisted of CNT sheets. When the strain was increased from 10% to 50% under a 10-Hz movement, this sensor demonstrated an increase of voltage from 13 to 24 mV, current from 3 to 8 nA, and charge from 5.5 to 10 pC. A TENG sensor consisting of multiple such fibers was constructed by weaving and demonstrated in sensing mechanical stretch and bending.

Gong et al. (2017) developed a wearable kinematic sensor based on a stretchable core-sheath structured yarn. A conductive metal core fiber was covered with nylon fibers (Figure 5E), and they acted as the electrode and positive triboelectric surface, respectively. This was placed inside a silicone rubber tube, which acted as the negative triboelectric layer. A bamboo fiber/Ag nanowire coating was deposited on the outside of silicone tube, which acted as the other electrode, with a layer of PDMS being deposited as the outermost layer of the structure. This device was demonstrated for human motion monitoring, capable of identifying characteristic walking patterns when connected as a knee pad.

Apart from core-shell structures, conductive and non-conductive fibers can be twisted or blended to produce TENGs. For instance, Zhou et al. developed a twisted fiber TENG (Figure 5F) for wearable applications by twisting cotton threads modified with CNT and PTFE. Cotton thread was coated with CNT using dip coating, obtaining even loading of ~0.207 mg/cm and a conductivity of 1.552 mS/cm (Zhou et al., 2014a, 2014b). An additional coating of PTFE was applied on some of these yarns, and these two sets of yarns were twisted to construct the TENG, in which CNT and PTFE acted as triboelectric contact surfaces. This device produced an output power density of ~0.1 $\mu W/cm^2$ using finger motion, through a load of 80 MΩ. When combined into a woven fabric and sewn into a laboratory coat, the TENG was able to charge a 2.2 μF capacitor up to 2.4 V in 27 s, under shaking movement.

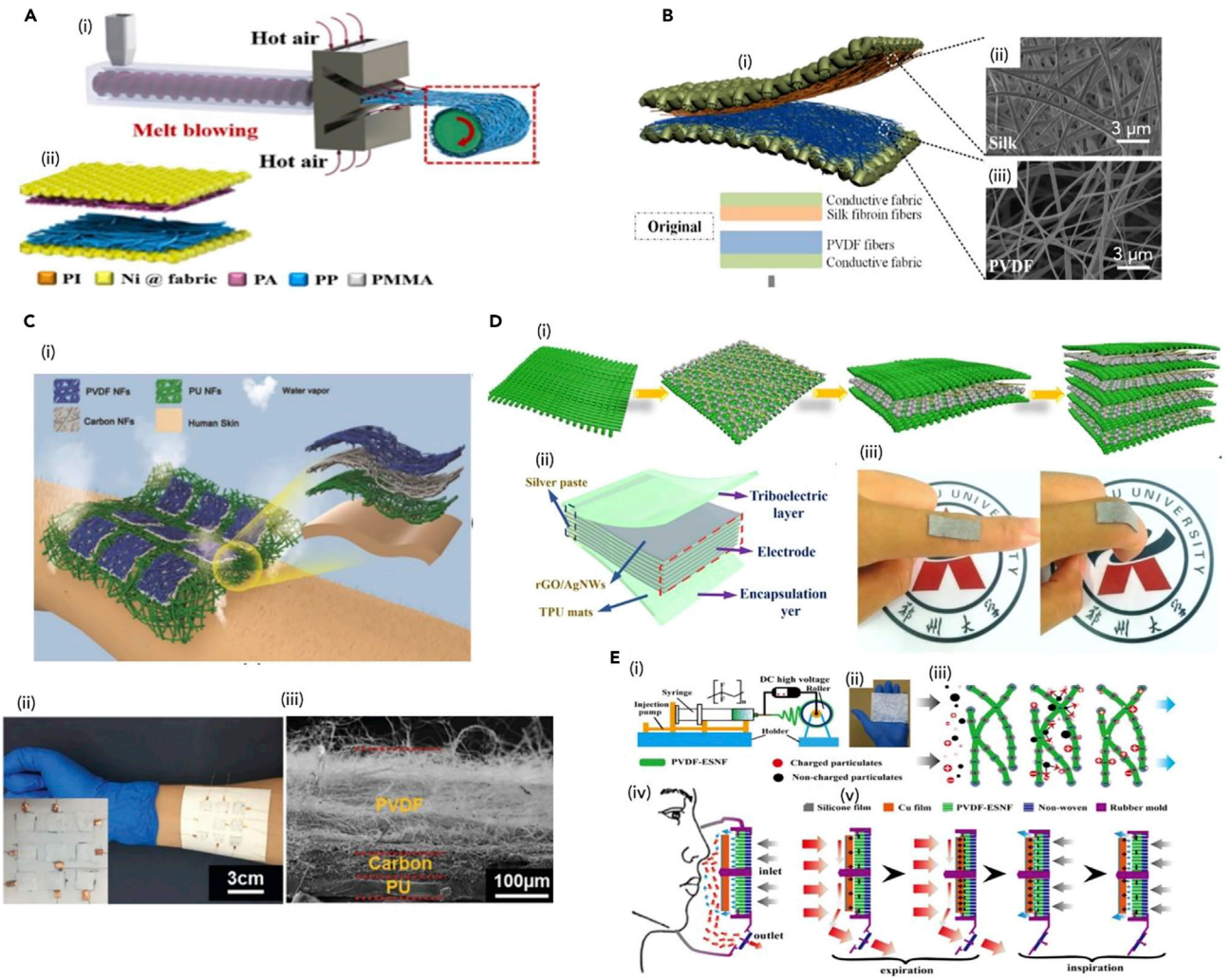


**Figure 6. Sandwiched Fiber/Yarn Based TENG Developments**

(A) Schematic of the (i) fabrication process and (ii) the structure of a nonwoven fabric-based TENG. Reprinted from ref (Peng et al., 2019) with permission, Copyright©2019 Elsevier Ltd.

(B) (i) Schematic of a piezoelectric/triboelectric hybrid nanogenerator constructed using electrospinning. Corresponding scanning electron microscopic (SEM) images of (ii) silk nanofibers and (iii) PVDF nanofibers. Reprinted from ref (Guo et al., 2018) with permission, Copyright©2018 Elsevier Ltd.

(C) (i) Schematic illustration of SETENG with PVDF and PU nanofibers, (ii) optical photograph of TENG on hand skin, (iii) SEM image of the cross-sectional view of fiber-based developed TENG device. Reprinted from ref (Li et al., 2020) with permission, Copyright©2019 WILEY-VCH Verlag GmbH & Co.

(D) Schematics of a TENG with a layered arrangement of AgNW, reduced graphene oxide, and thermoplastic PU, representing (i) the development process and (ii) the structure. (iii) A photograph of the final device. Reprinted from ref (Zhou et al., 2020) with permission, Copyright©2020 Elsevier Ltd.

(E) Construction and working mechanism of a TENG-based face mask, demonstrating (i) schematic of electrospun PVDF nanofiber fabrication, (ii) photograph of the electrospun PVDF nanofibers, (iii) schematic of filtration mechanism of the nanofibers, (iv) schematic of the structure of the facemask, and (v) schematic of the operation of the TENG-based facemask during expiration and inspiration. Reprinted from ref (Liu et al., 2018a, 2018b) with permission, Copyright©2018 American Chemical Society.

## Sandwiched Fiber/Yarn-Based TENGs

Sandwiching fibers or yarns between multiple material layers has been a common strategy used for textile-based TENGs. One of the key advantages is that the fiber webs, which may not have the required rigidity and durability (e.g., nanofibers or nanomaterials), can be easily incorporated into TENGs with this method. Electrospun fiber webs have been a key feature in sandwiched fiber-based TENGs.

Among examples for this category, Peng et al. (2019) developed a TENG based on melt-blown nonwoven fabric for energy harvesting and self-powered sensing (Figure 6A(i)). This device consisted of nonwoven

polypropylene (negative triboelectric surface) and nylon 6,6 (positive triboelectric surface) fabric layers sandwiched between Ni-coated nylon fabrics (electrodes) (Figure 6A (ii)). The optimum output performances of the device were recorded as a peak $V_{OC}$ of 210 V, $J_{SC}$ of 28.3 $\mu A/m^2$, and $Q_{SC}$ of 97.3 nC under 6-Hz frequency contact separation movement, for a 60 × 60 $mm^2$ surface area. The peak power density of 901.7 $mW/m^2$ was generated through a 70-MΩ resistor. This device was used to charge a 1-μF capacitor to power a digital watch and 124 light-emitting diodes (LEDs) by hand tapping. Furthermore, the device was demonstrated for sensing applications, as a pedestrian volume collector and a training monitor.

A hybrid piezoelectric and triboelectric fiber-based TENG was developed by Guo et al. (2018) (Figure 6B). This device contained silk fibroin and PVDF nanofibers as the two triboelectric surfaces, which were electrospun onto conductive fabrics electrodes. The fiber-based development showed high active surface area and air permeability and was capable of being embedded into garments. The peak outputs indicated a $V_{OC}$~500 V, $I_{SC}$~12 μA, and power density 310 $\mu W/cm^2$ through a 100 MΩ load when subjected to hand tapping at 2 Hz frequency. This device was used to develop a self-powered real-time fall alert system, demonstrating its practical usage.

A number of single-electrode-mode fiber-type sandwiched TENGs have also been developed. Li et al. (2020) presented a SETENG using carbon nanofibers (electrode) sandwiched between PVDF nanofibers (triboelectric sensing layer) and PU nanofibers (substrate layer) (Figure 6C). In contact with the skin, the PVDF acquires a negative charge where the skin charges positively, providing the triboelectric charging for the device to operate. This device achieved a peak power density of 85.4 $mW/m^2$ through a load of 50 MΩ, under 140 kPa pressure. As a pressure sensor, this device demonstrated a sensitivity of 0.18 V/kPa in the range between 0 and 175 kPa, retaining almost constant sensitivity up to 50% elastic deformation. An array of these energy harvesters (4 × 4 $cm^2$) were used to illuminate 50 LEDs by hand tapping, while wearing a glove.

In another example, Zhou et al. (2020) developed a nanofiber-based sandwiched TENG by spraying multiple layers of AgNW and a reduced graphene oxide mixture (electrode) on to thermoplastic PU nanofiber mats (triboelectric surface) (Figure 6D). This device operated in SETENG mode, using skin as the counter-triboelectric layer. The device generated maximum $V_{OC}$~202.4 V and instantaneous power density of 6 $mW/m^2$ through a 400 MΩ load, when subjected to a movement of 10 Hz, under 10 N contact force. The output performances were stable up to 200% strain. As a pressure sensor, this device exhibited a sensitivity of 78.4 V $kPa^{-1}$ in the 0–2 kPa range, along with a 1.4 ms response time. A tactile sensor array (5 × 5) consisting of the TENG units (1 ×1 $cm^2$) was demonstrated to monitor finger motion trajectory.

In a different device architecture, Liu et al. (2018a, 2018b) constructed a TENG-based self-powered electrostatic adsorption face mask (Figure 6E). An electrospun PVDF nanofiber layer was deposited on the nonwoven substrate, which acted as the negative triboelectric surface. A Cu film was placed opposite to the nanofiber layer to act as the positive triboelectric surface, creating a sandwiched TENG structure. When integrated into a face mask, the inhalation and exhalation actions cause the triboelectric surfaces to contact and separate, which results in triboelectric charging of the two surfaces. According to theoretical simulations, the contact and separation of these triboelectric surfaces resulted in a potential difference of ~2 kV. The TENG-based face mask demonstrated removal efficiencies of 99.2 wt % for coarse and fine particulates and 86.9 wt % for ultrafine particulates, after continuously wearing for 4 h and a 30 day interval.

## Optimization Methods for Fiber/Yarn-Based TENGs

The fiber- and yarn-based TENG developments discussed earlier in the article used a number of output optimization strategies in material selection and device fabrication, which will be discussed here, in relation to increasing the triboelectric charge density (discussed in Figure 2C) and improving the electrostatic induction (discussed in Figures 2D–2H).

Considering the charge density improvement, material selection has been a key focus point. Selecting materials further apart in the triboelectric series to obtain higher triboelectric charge separation has been a major strategy (e.g., polyester and nylon, Liu et al., 2019a, 2019b; silver and PU, Sim et al., 2016). Moreover, physical and chemical modification of triboelectric fiber/yarn surfaces has been conducted to enhance triboelectric charging. These methods include modifying the triboelectric fibers/yarns by incorporating nanomaterials and nanofibers to improve triboelectric contact areas (Cheon et al., 2018; Guo et al.,

2018; Li et al., 2020; Ma et al., 2020; Zhou et al., 2020) and developing composite materials-related triboelectric fibers and yarns (Kim et al., 2020). Furthermore, fiber-type TENG architectures have been designed to facilitate improved contact between the triboelectric surfaces. For instance, some devices have been constructed with materials such as PU (Sim et al., 2016; Yu et al., 2017; Zhou et al., 2020) and PDMS (Gong et al., 2017; He et al., 2017), which provide conformal properties during contact and desirable frictional characteristics.

Several output optimization methods have been used to improve electrostatic induction. Controlling the thickness of the dielectric layer of fiber-type TENGs, especially in core-shell device architectures, has been shown to increase the electrical outputs (Gong et al., 2019a, 2019b). Similarly, larger TENG surfaces were shown to increase the output performances (Li et al., 2020). The importance of dielectric constant during material selection and environmental conditions such as the medium in which the TENGs are operating, toward enhancing TENG outputs, has been highlighted in fiber-based TENG studies (Gong et al., 2019a, 2019b). The motion parameters critically affect the output enhancement to fiber-type TENGs, where increasing the operating frequency and amplitude of the TENG increased the current, voltage, and power outputs (Li et al., 2020; Zhou et al., 2020).

## Future Perspectives of Fiber/Yarn-Based TENGs

Early fiber/yarn-based TENG developments used traditional textile materials (cotton, Zhou et al., 2014a, 2014b; nylon, Gong et al., 2017) and rigid structures in synergy to enhance the power output of wearable TENGs, with less focus on wearer comfort. However, more recent TENG developments focused on obtaining improved performances in both electrical and wearable aspects. For instance, some developments focused on flexible TENG designs with core-shell architectures, using soft core filaments (He et al., 2019; Lou et al., 2020; Ye et al., 2020a) and micro-fibrous shell materials (Ma et al., 2020), as opposed to conventional rigid metallic filaments. Several of these devices (Lou et al., 2020; Yu et al., 2017) showed acceptable levels of washability, although other important wearable properties like moisture management and breathability are yet to be investigated. There has been an increasing interest in using nanofibrous structures to enhance the surface area of sandwich-structured TENGs, which act favorably on moisture management properties (e.g., water vapor transmission rate of 10.26 kg $m^{-2}d^{-1}$) and air permeability (Li et al., 2020; Zhou et al., 2020). TENGs that utilize thin coatings using atomic deposition methods have been fabricated; however, these coatings exhibited poor washability and low mechanical robustness (Zhou et al., 2014a, 2014b). Tailorability is another important parameter that governs the wearability of textile-based TENGs. Several studies have shown interest in addressing tailorability by using core-shell structured yarns (Ye et al., 2020a; Yu et al., 2017) and sandwiched device structures (Guo et al., 2018).

Many textile-based TENG developments so far have been limited to laboratory scale, with significant pragmatic concerns to be addressed before scaling up or commercialization. One of the main concerns is the compatibility of conventional large-scale fiber/yarn manufacturing techniques with the intricate designs of TENG designs developed so far, which will massively benefit the scaling up of this technology. Therefore, it is important for TENG developers to be aware of the general requirements and guidelines of the techniques and machinery used in the fiber/yarn spinning industry. Almost all wearable developments based on triboelectric fibers/yarns are finally integrated into garments via fabric manufacturing processes of weaving or knitting, or are nonwoven, and subjected finally to sewing. Herein, the yarn diameter becomes a critical parameter. Considering weaving, the yarn diameters should be compatible with the weft insertion mechanism and machine type in the commercial weaving processes. The yarn diameter is also an important factor in the knitting process where the knitting ability depends on the insertion of triboelectric yarn into the knitting needles. Furthermore, due consideration of the "gauge" (the number of needles per unit length) of knitting machines is of paramount importance for the compatibility of triboelectric yarns with the knitting process. Other important parameters/requirements of both weaving and knitting processes are yarn uniformity, flexibility, and high tensile strength (Adanur, 2000; Ahmad et al., 2017; Spencer, 2001). As a guideline, a summary of the critical yarn requirements for common commercial fabric manufacturing processes is provided in Note S4. Tailorability of triboelectric yarns requires meeting sewing requirement such as strength, abrasion resistance, low shrinkage, etc. Note S5 consists of a summary of such parameters (Ahmad et al., 2017).

A number of yarn processing techniques used in the textile industry can be applied for the fiber/yarn-type TENG developments and their output enhancement. Mechanical structural design (MSD) is a prominent

method that could potentially be used to enhance triboelectric charge density (Dharmasena and Silva, 2019a, 2019b) by increasing the surface roughness and surface features of the fibers and yarns. MSD can be applied for yarn processing techniques such as drawing, plying, twisting, texturing, spinning, and covering, which can be adapted for TENGs (Lawrence, 2010; Zhang, 2014). For instance, air jet texturing is a method of creating bulky yarns (Sengupta et al., 1995) from synthetic filaments, which significantly enhances their hand feel, comfort, and surface features (Acar et al., 2006). Partially drawn yarn can be used in the texturing process to increase the bulkiness and the surface area by introducing extra length of loops and neps into the yarn, which could enhance TENG output performances (Cayuela et al., 2012; Choi and Kim, 2015; Sengupta et al., 1995). Yarn covering is another process used in the textile industry to wind a cover yarn around a stretchable or conductive core yarn, and this process has the potential to develop improved core-axial materials for TENGs (Petrulis and Petrulyte, 2009; Yoshimura et al., 1969). For instance, hollow spindle covering is a well-known method to produce single- and double-covered yarns. Such processes would provide high yarn uniformity (Park et al., 2018), higher surface area (Asghar et al., 2019; Wang et al., 2015a, 2015b, 2015c, 2015d), better moisture management, and air permeability (Lawrence, 2010; Wang et al., 2015a, 2015b, 2015c, 2015d), which will significantly enhance electrical and wearable output performances of fiber/yarn-based TENGs.

## FABRIC-RELATED TENG DEVELOPMENTS

Textile-based TENG developments in which the major triboelectric functionalization occurred in the fabric stage (processes depicted in Figures 3E–3Q) are categorized as fabric-related TENGs in this work. Fabrics have been used as triboelectric layers, electrodes, and/or the substrates of TENGs (Paosangthong et al., 2019a). Compared with fiber- and yarn-based TENGs, developing wearable TENGs in the fabric stage facilitates convenience in handling, fabrication, and functionalization. However, the construction of high-performing fabric TENGs while retaining esthetic and wearable properties has been challenging. Fabric-based TENGs are divided into three categories based on their structure and manufacturing method: woven, knitted, and nonwoven-based TENGs. Note S6 summarizes some of the significant wearable TENG developments, based on common fabric structures.

### Woven Fabric-Related TENGs

Woven fabric-related TENGs are the most common type among fabric-based TENGs (Chen et al., 2020, 2018; Liu et al., 2020a, 2020b; Lou et al., 2020; Ning et al., 2018; Pu et al., 2016b, 2016a; Shi et al., 2017). This section discusses woven fabric-related TENGs in which the major triboelectric functionalization took place during or after the weaving process. Such devices are analyzed under two categories depending on the functionalization method, namely, surface modified and structurally modified woven fabric TENGs.

#### *Surface-Modified Woven Fabric-Based TENGs*

Woven fabrics can produce even and closely bound fabric surfaces for TENG fabrication. Therefore, they have been utilized as substrates or triboelectric interfaces, often in combination with nano/micro-structured surface modifications applied chemically or mechanically to improve contact area and frictional properties, targeting to enhance the triboelectric charge density (Ko et al., 2015; Lee et al., 2015; Pu et al., 2015; Seung et al., 2015; Xiong et al., 2018).

Among examples in this category, Lee et al. (2015) developed a TENG using a gold (Au)-coated woven textile (7 × 7 $cm^2$), aluminum (Al) nanoparticles, and PDMS (Figure 7A). To create the top TENG layer, Al nanoparticles (triboelectric surface) were grown on the top of an Au-coated textile (electrode). Bottom TENG layer was produced by spin coating PDMS (triboelectric surface) over an Au-coated textile, followed by reactive ion etching, which created a nanostructure with 150 nm diameter and 2.5 μm height. The device generated a maximum $V_{OC}$ of 368 V and $I_{SC}$ of 78 μA by bending at 100 mm/s and 3 cm bending length. A maximum power density of 33.6 mW/$cm^2$ was achieved through a 20 Ω load, under a 20 mm/s operation speed and 3 cm length. Attached onto an arm sleeve, the TENG was used to light up several LEDs using bending and releasing motion.

An oblique PDMS microrod array-based TENG was developed by Zhang et al. (2019), for wearable energy harvesting (Figure 7B). In this structure, the top TENG layer was prepared with a nylon woven fabric by printing carbon paste on one side (electrode) and using reactive ion etching to create evenly distributed nanowires (diameter of 30–50 nm) (triboelectric surface) on the other side. PDMS microrods (25 μm diameter,

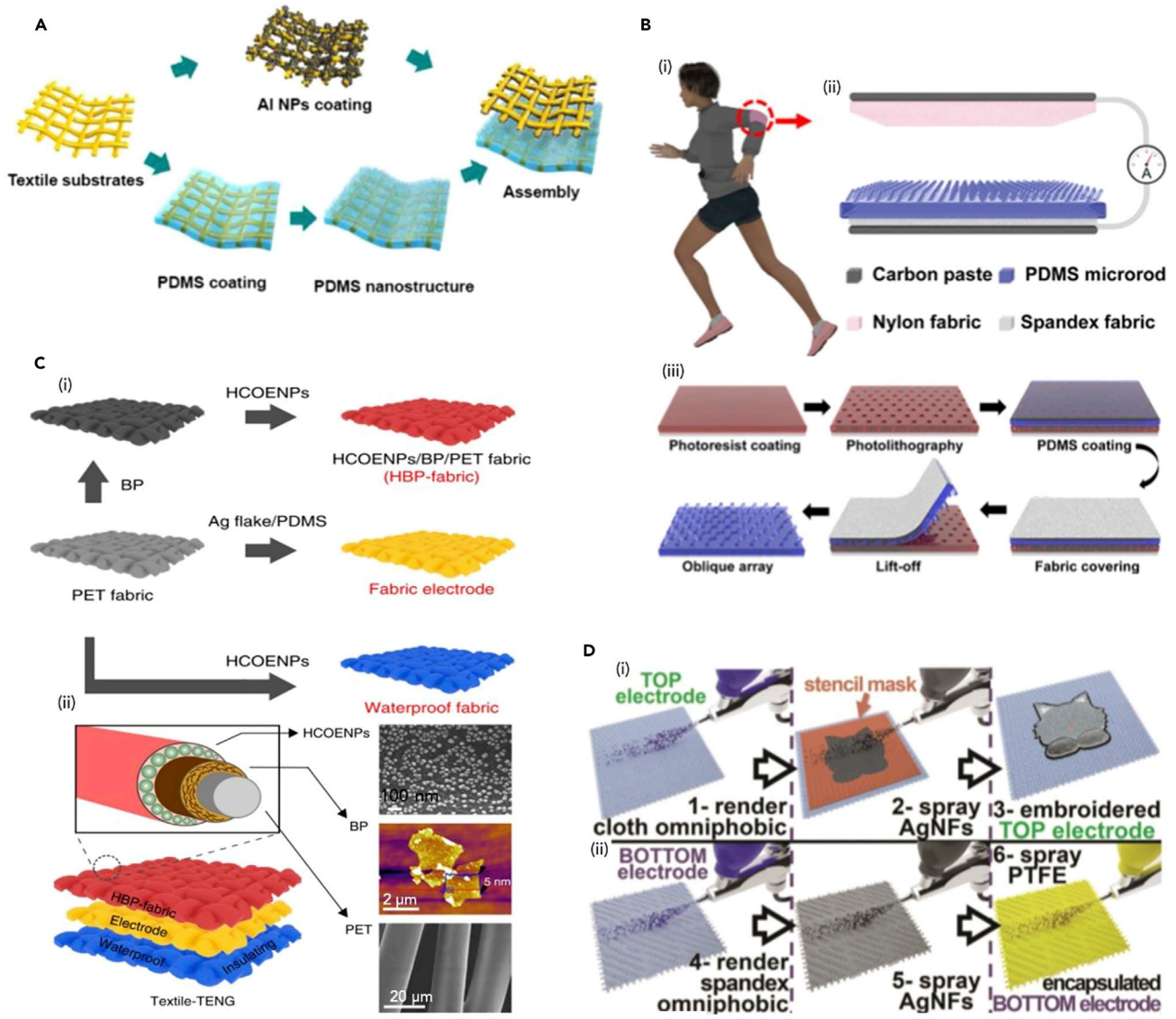


**Figure 7. Surface Modified Woven Fabric Based TENG Developments**

(A) Schematic of a TENG fabrication flowchart for a nanostructured surface geometry. Reprinted from ref (Lee et al., 2015) with permission, Copyright©2015 Elsevier Ltd.

(B) (i) Design of TENG to harvest energy from human motion, (ii) schematic diagram of the TENG structure, and (iii) PDMS microrod array fabrication process on a spandex fabric. Reprinted from ref (Zhang et al., 2019) with permission, Copyright©2019 American Chemical Society.

(C) (i) The fabrication process of TENG consisting of a PET fabric with black phosphorus, Ag flakes, PDMS, and encapsulated hydrophobic cellulose oleoyl ester nanoparticles and (ii) a schematic of the TENG device. Reprinted from ref (Xiong et al., 2018) with permission, Copyright©2018 Springer Nature.

(D) (i) Flowchart for top TENG layer and (ii) bottom TENG layer for an omniphobic TENG. Reprinted from ref (Sala de Medeiros et al., 2019) with permission, Copyright©2019 WILEY-VCH Verlag GmbH & Co.

30 μm length, 30° inclined) (triboelectric surface) were structured over a spandex fabric (containing carbon paste as the electrode), using lithography and template transfer techniques (Figure 7B (ii)), which was used as the bottom TENG layer. This device recorded a $V_{OC}$ of 1,014.2 V, $J_{SC}$ of 3.24 μA/cm$^2$, and charge density of 10.28 nC/cm$^2$, under 5 Hz frequency and 10 mm amplitude movement (30% humidity at 16°C). Furthermore, a maximum power density of 211.7 μW/cm$^2$ was reached through a 6 MΩ load, and 48 commercial red LED bulbs connected in series were lit up simultaneously using continuous hand tapping.

Some recent woven fabric TENGs have focused on wearable properties such as air permeability and washability alongside power enhancement. For example, Xiong et al. (2018) developed a TENG by applying black phosphorus-encapsulated hydrophobic cellulose oleoyl ester nanoparticles on PET fabric (HPB fabric, triboelectric layer), along with a waterproof fabric and a fabric electrode (Figure 7C). The static contact angle of 1.53° for the SETENG structure ensured superior hydrophobic properties over the fabric. This device also showed 1,068 $\pm$ 3 L $m^{-2}$ $s^{-1}$ air permeability. Using skin as the secondary triboelectric layer, the TENG generated peak $V_{OC}$ of 880 V and $J_{SC}$ of 1.1 $\mu A/cm^2$ under hand touching, which exerted a 5 N force at 6 Hz frequency. This device generated a power density of 0.52 $mW/cm^2$ through a 100 M$\Omega$ load, and 150 LED bulbs were illuminated through hand tapping movements (<5 N, 4 Hz).

Sala de Medeiros et al. (2019) developed an omniphobic TENG by combining embroidery and spray deposition of conductive nanoflakes, PTFE, and fluoroalkylated organosilanes, in a twill woven fabric substrate. Herein, the top TENG layer was prepared (Figure 7D (i)) by spraying fluoroalkylated organosilanes (to obtain omniphobic properties and act as a triboelectric surface) followed by Ag nanoflakes (electrode) on a laser-cut stencil to create the required design. This layer was protected by embroidering a shape matching design on the top. In the bottom layer (Figure 7D (ii)) a spandex fabric was treated for omniphobic properties and then sprayed with Ag nanoflakes (electrode) followed by a PTFE layer (~8 $\mu$m) (triboelectric layer). The device demonstrated flexibility, lightweight, and air permeability of ~90.5 mm/s. When the two triboelectric layers were combined (device size 6.25 $cm^2$), peak $V_{OC}$ of 300 V and $I_{SC}$ of 80 $\mu$A was generated by two fingers tapping at 4 Hz frequency. The maximum power density of 600 $\mu W/cm^2$ was recorded from this device, through a 1 M$\Omega$ load. The device was attached into the collar of a shirt to the control volume, pause, and resume functions of a music player integrated into the textile.

### *Structurally Modified Woven Fabric-Based TENGs*

Some of the woven fabric-based TENGs have been constructed using fabric structural modifications, which include woven pattern variations (Chen et al., 2020, 2018; Ma et al., 2020; Ning et al., 2018; Zhao et al., 2016a, 2016b; Zhang et al., 2016), grated fabric structures (Paosangthong et al., 2019b; Pu et al., 2016b), corrugated structures (Choi et al., 2017), wrinkled structures (Liu et al., 2020a, 2020b) etc., which we discuss in this section. Such modifications are viable during weaving because two different yarn sets (warp and weft) are being interlaced.

For instance, Zhang et al. (2016) developed a machine-washable TENG for human respiratory monitoring using shuttle weaving technology, which comprised a Cu/PET yarn structure (~300 $\mu$m diameter) as warp yarns and PA-coated Cu/PET yarn structure (~350 $\mu$m diameter) as weft yarns (Figure 8A (i)). When subjected to tapping motion at 10 cm/s, the device produced a peak $V_{OC}$ of 4.98 V, $J_{SC}$ of 15.50 $mA/m^2$, and maximum power density of 33.16 $mW/m^2$ through 60 M$\Omega$ load. This device indicated air permeability of 0.17 $\pm$ 0.03 kPa s/m and good washability. The TENG was used to obtain respiratory rate and depth information, being used as a self-powered respiratory monitoring device. In addition, a theoretical platform was constructed to relate woven fabric parameters with the electrical performances of the TENG (Figure 8A (ii–v)), which will be further discussed in the section Optimization Methods for Fabric-Based TENG Devices.

Utilizing more advanced weaving techniques, Dong et al. (2017a) developed a 3D orthogonal woven structure, consisting of 2D plain fabrics (stainless-steel warp/PDMS-coated stainless-steel weft) connected by non-conductive binding yarns (z-yarn) (Figure 8B (i and ii)). Compared with a 2D plain-woven fabric, the 3D structure provided enhanced surface area, allowing the generation of high surface charges along with improved breathability, flexibility, and comfort. This device (area 45 × 40 $mm^2$) generated a peak $V_{OC}$~45 V, $I_{SC}$~1.8 $\mu$A, and charge~18 nC under 5 Hz frequency and 25-mm-amplitude tapping movement. A power density of 263.36 $mW/m^2$ was achieved through a 132 M$\Omega$ load when the device was subjected to 3-HZ movement, and a 0.68-$\mu$F commercial capacitor was charged to 2.5 V within 7 s by hand tapping.

The structural modification capability of woven TENGs has been demonstrated to address inherent performance issues of TENG technology such as their power management. For example, Chen et al. developed an energy harvesting and storage integrated woven textile (Figure 8C (i)) (Chen et al., 2018) using shuttle weaving. In this FSTENG-based energy harvester, the dielectric woven fabric was constructed using cotton in the warp direction, with cotton and PTFE yarns inserted selectively as the weft. The electrode of this device was woven by using cotton in the warp direction, whereas cotton and carbon fiber yarns were inserted selectively as the weft. Different carbon fiber electrode segments were connected through loads to

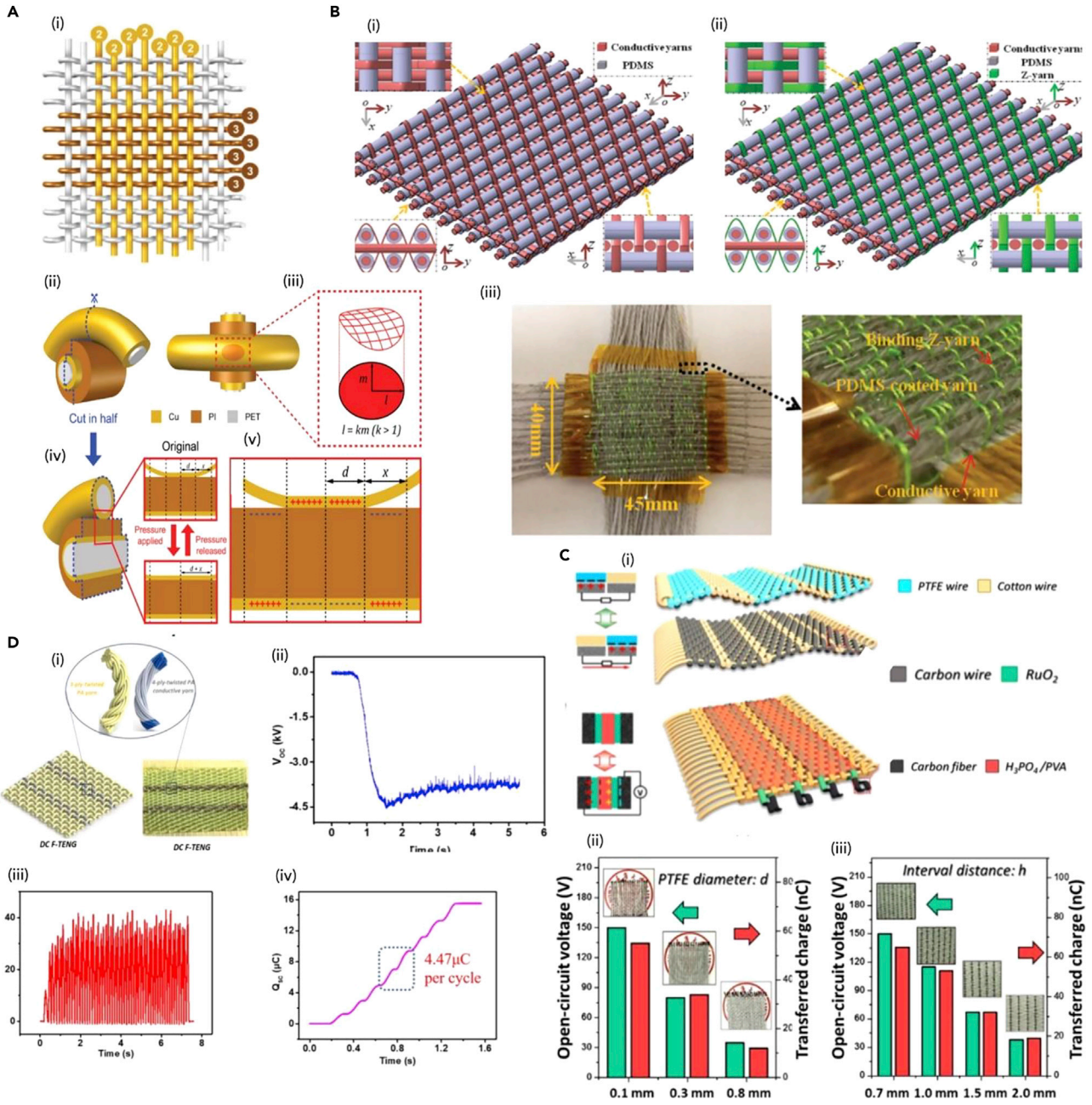


**Figure 8. Structurally Modified Woven Fabric Based TENG Developments**

(A) (i) Schematic of Cu-PET yarn-based woven TENG structure and illustration related to the woven TENG theoretical model development showing (ii) the side and top views of yarn interlacing, (iii) morphology of the contacting interlacing, (iv) cross-sectional view of the yarn interlacing point when pressure is applied (top) and released (bottom), (v) charge distribution at yarn interlacing point when contacting area changes. Reprinted from ref (Zhang et al., 2016) with permission, Copyright©2016 WILEY-VCH Verlag GmbH & Co.

(B) Fabrication process of the 3D orthogonally woven TENG, depicting (i) conductive and (ii) nonconductive z-direction yarn binding. (iii) Photograph of 3D woven TENG, Reprinted from ref (Dong et al., 2017a) with permission, Copyright©2017 WILEY-VCH Verlag GmbH & Co.

(C) (i) Schematic of a woven TENG, demonstrating the dielectric component, electrode component, and energy storage unit. The output variation of the TENG against (ii) increasing PTFE yarn diameter and (iii) the interval distance between the yarns. Reprinted from ref (Chen et al., 2018) with permission, Copyright©2018 Elsevier Ltd.

(D) (i) Schematic of the woven DC TENG and the corresponding electrical outputs depicting (ii) $V_{OC}$, (iii) $I_{SC}$, (iv) $Q_{SC}$. Reprinted from ref (Chen et al., 2020) with permission, Copyright©2020 American Chemical Society.

harvest output energy, generated through relative movement between the dielectric fabric layer and the electrode fabric layer. A supercapacitor woven fabric was constructed using cotton yarns in the warp direction, and the weft consisting of carbon fiber yarn electrodes, $RuO_2$-coated carbon fiber yarns (separated by cotton threads), and PVA/$H_3PO_4$ gel electrolyte-coated carbon fiber yarns. The TENG device, subjected to 20 cm/s sliding speed, generated a peak $V_{OC}$~118 V, $I_{SC}$~1.5 μA, and charge of 48 nC. The output characterization indicated improved performance at low yarn diameters (Figure 8C (ii)) and low weft yarn gaps (Figure 8C (iii)), potentially due to increased cover factor of the fabric. This device was stitched on to a hand glove, and the rubbing and patting movements were used to illuminate 18 LEDs.

Similarly, Chen et al. (2020) developed direct current (DC) woven fabric TENG to address discontinuity of electrical outputs of a textile-based TENG, along with improved wearable properties. In this woven structure, three-plied twisted nylon 6,6 was used as warp yarns. The weft consisted of two types of yarns, nylon non-conductive yarns, and nylon conductive yarns with an Ag coating, which were separated as two electrodes (electrostatic breakdown yarns [0.4 mm diameter] and frictional yarns [0.52 mm diameter]) (Figure 8D (i)). The area density of the fabric was 326 g/$m^2$. With the combined effect of electrostatic induction and electrostatic breakdown effects, this device produced DC outputs for voltage (Figure 8D (ii)), current (Figure 8D (iii)), and charge (Figure 8D (iv)). The device (6.8 × 7 $cm^2$) generated a peak $V_{OC}$ of 4,500 V, $I_{SC}$ of 40 μA, and short circuit charge ($Q_{sc}$) of 4.47 μC, by moving a PTFE film over the device at 0.01 m/s for a moving distance of 20 mm, with a weight of 1 kg. A yarn-based supercapacitor was constructed using two sets of carbon fiber (electrode)-coated with Nafion, poly(3,4-ethylenedioxythiophene) polystyrene sulfonate (PEDOT:PSS), and solid-state $H_3PO_4$/PVA gel electrolyte along with this TENG device. The outputs from the small size TENG (1.5 cm × 3.5 cm) was used to light up 416 LEDs (serially connected).

### Knitted Fabric-Related TENGs

Knitted fabrics are gaining increasing popularity in constructing fabric-type TENGs, due to its improved wearable and comfort characteristics such as high stretchability and breathability (Spencer, 2001). Using three main stitch types, knit stitch, tuck stitch, and miss stitch (Figure 9A), and combining different interlooping patterns, a wide variety of knitted fabric types are constructed at present (Spencer, 2001). The majority of knitted fabric TENGs developed so far focused on weft-knitted structures (Figure 4E), which include 2D as well as 3D knitted structures (Dong et al., 2017b; Huang et al., 2019; Kwak et al., 2017).

Considering 2D knitted examples, Huang et al. (2019) developed an FSTENG (Figure 9B (i)) using a simple plain knit. One of the triboelectric layers (9 × 10 $cm^2$) consisted of Ag-coated nylon yarns (positive triboelectric surface and electrodes) and cotton yarns (separating the electrodes). The counter triboelectric layer (9 × 5 $cm^2$) was constructed using a PTFE membrane (triboelectric surface) attached to a polyester fabric. The sliding movement between the two TENG layers was used to generate power (Figure 9B (ii)), exhibiting acceptable air permeability (884.78 mm/s), washability, and flexibility for wearable applications. Different fabric textures of the knitted fabric (technical front and back sides) were investigated with regard to output performances, with the highest performance of the TENG being a peak $V_{OC}$ of 900 V, $I_{SC}$ of 19 μA, and a peak power density of 203 mW/$m^2$ (through an 80-MΩ resistor), obtained using a simple swinging motion. The applicability of this device for powering electronics was demonstrated by lighting up 51 LEDs using arm swinging motion.

In a relatively complicated design, Fan et al. (2020) constructed a knitted TENG sensor array using a stainless-steel/terylene twisted yarn (electrode and negative triboelectric layer) and a nylon yarn (positive triboelectric layer) plated together, in a full cardigan knit (Figure 9C (i)). The device was fabricated using a double bed flat knitting machine, where the conductive and nylon yarns were tucked alternatively in front and back needle beds, obtaining a complete plating rather than a point contact. The capability of this architecture in pressure sensing was investigated while varying the yarn parameters. Among different yarn parameters, 210D/3 (3 plied, 210 deniers) conductive yarn along with 210D/6 (6 plied, 210 deniers) nylon yarn provided the best output performances, demonstrating pressure sensitivity of 7.84 mV/Pa up to 4 kPa and sensitivity of 0.31 mV/Pa thereafter. The device demonstrated fast response time (20 ms) in 1–5 Hz frequency range, under 1 kPa pressure. Applicability of this device in self-powered epidermal physiological monitoring was demonstrated by sensing pulses from the neck, wrist, fingertip, and ankle (Figure 9C (ii and iii)).

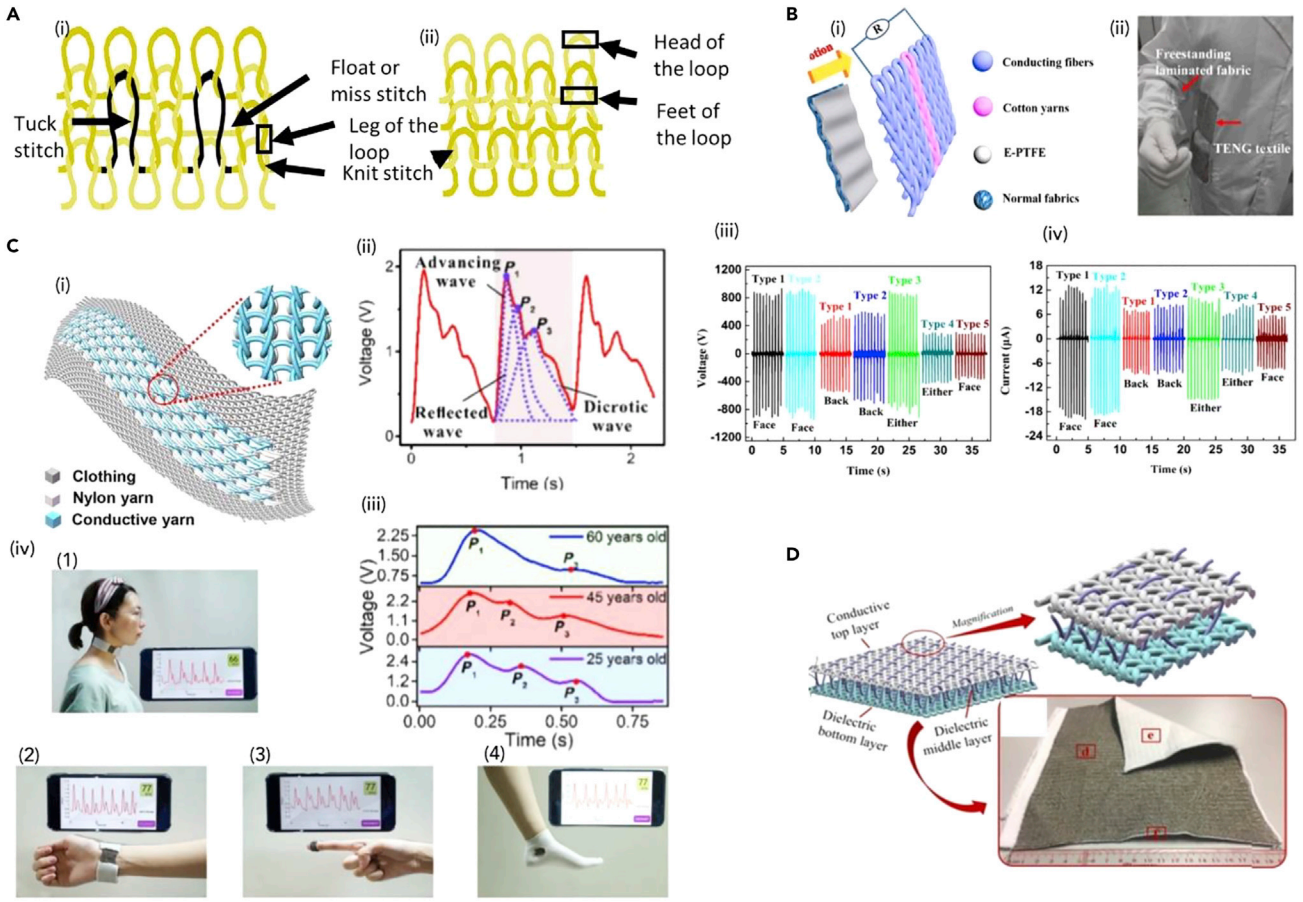


**Figure 9. Knitted Fabric Based TENG Developments**

(A) Schematic of knitting stitch types of a weft-knitted fabric on the (i) technical front and (ii) technical backsides, adopted from ref (Spencer, 2001).

(B) (i) Schematic of the structure of a 2D knitted TENG and (ii) a photograph of the TENG attached to a laboratory coat. The output characterization of the 2D knitted TENG, demonstrating (iii) voltage and (iv) current against time, for several knitting variations. Reprinted from ref (Huang et al., 2019) with permission, Copyright©2019 Elsevier Ltd.

(C) Schematic of the cardigan structure-based knitted TENG. Outputs from the knitted TENG demonstrating (ii) pulse of the neck of a person and (iii) comparison of pulse waveforms of persons at different ages. Reprinted from ref (Fan et al., 2020) with permission, Copyright©2020 The Authors.

(D) Schematic of the structure of a 3D knitted fabric-based TENG (top) and a photograph of the device (bottom). Reprinted from ref (Gong et al., 2019a, 2019b) with permission, Copyright©2019 Elsevier Ltd.

Several 3D knitted TENG fabrics have been reported for energy harvesting and sensing purposes. For example, Gong et al. (2019a and 2019b) developed a wearable TENG based on 3D knitting (spacer fabric) techniques, which operated in the SETENG working mode (Figure 9D). Herein, Ag-coated nylon yarns were used to knit the top fabric, which acted as the electrode as well as the positive triboelectric surface. A PAN-based yarn was used to construct the bottom fabric, acting as the negative triboelectric surface. Cotton was used as the spacer yarn, which connected the top and bottom fabrics, creating a 1-mm spacer gap. In terms of comfort properties, the device indicated an improved thermal conductivity of $8.35 \times 10^{-2}$ $Wm^{-1}$ $K^{-1}$ (higher than cotton) and high air permeability of 0.834 kPa s/m. During performance characterization, a PDMS film was used as a triboelectric element to contact and separate with respect to the conductive layer, and under a contact force of 1,200 N, the device generated a maximum power density of 1,768.2 $mW/m^2$ through a 50 MΩ load. This device was used to illuminate up to 320 commercial LEDs, and to charge a 200-μF commercial capacitor at a rate of 11.3 mV/s.

## Nonwoven Fabric-Related TENGs

Being a relatively innovative manufacturing method, nonwoven fabrics provide advantages such as ease of fabrication and scaling up, fast production rates, and compatibility with a large variety of fiber types.

Although not being as popular as woven or knitted developments, limited number of nonwoven-related TENG designs have been presented in the literature (Liu et al., 2018a, 2018b; Peng et al., 2019; Wang et al., 2019), which used the nonwovens as the substrate of the TENG architecture. We note that, in our categorization, these particular examples fall under sandwiched fiber-structured TENG category (section Sandwiched Fiber/Yarn-Based TENGs), as the main triboelectric modification took place at the fiber stage of the active materials. However, looking at the origin and the fast growth of nonwovens in the mainstream textiles industry, it is highly likely that nonwoven-based stand-alone TENG developments will be available in the near future.

## Optimization Methods for Fabric-Based TENG Devices

Analyzing fabric-based TENGs discussed in the sections Woven Fabric-Related TENGs, Knitted Fabric-Related TENGs, and Nonwoven Fabric-Related TENGs, several key optimization techniques can be identified. Among theoretical developments, Zhang et al. (2016) presented a set of equations to approximate voltage and current outputs of a woven fabric (Figure 8C (ii)–(v)). According to this model, increasing the triboelectric charge density and separation velocity and reduction of dielectric constant of the fabrics result in higher TENG outputs, agreeing with the DDEF model predictions (Figure 2). On the other hand, experimentally demonstrated optimizations for fabric-based TENGs can be related to triboelectric charge density improvements and electrostatic induction enhancements.

Considering charge density improvements, selecting triboelectric materials further apart in the triboelectric series has been a major focus (Chen et al., 2020, 2018; Liu et al., 2020a, 2020b; Lou et al., 2020; Ning et al., 2018; Pu et al., 2016b, 2016a; Shi et al., 2017). Furthermore, physical and chemical modifications of triboelectric materials and contact surfaces have also been successfully implemented in this regard. For instance, composite material structures have been used for fabric-based TENG developments, obtaining higher triboelectric charging (Bai et al., 2019; Guo et al., 2020; Liu et al., 2020a, 2020b). Similarly, constructing surface patterning on fabrics (Choi et al., 2017; Huang et al., 2019; Paosangthong et al., 2019b; Zhang et al., 2019) (e.g., grated or corrugated structures, reactive ion etching) and the use of nanomaterials and nanopatterning techniques to enhance triboelectric contact area (Lee et al., 2015; Xiong et al., 2018) were successfully implemented to improve triboelectric charge density, thus enhancing TENG outputs. Furthermore, charge density enhancements have also been achieved by increasing triboelectric contact area via improvements in fabric structure. Some of such methods include designing fabrics using rough fibers with surface features (e.g., natural fibers) (Zhang et al., 2016), stretchable fabrics (e.g., 2 × 2 rib knit) (Kwak et al., 2017), fabrics with longer floating yarns (e.g., twill weave) (Somkuwar et al., 2020), 3D fabrics with larger surface areas (e.g., 3D weaving/knitting) (Dong et al., 2017a; Zhu et al., 2016a, 2016b), and multiple stacked fabric structures (Ko et al., 2015). For a given fabric, increasing the cover factor and surface roughness enhances the triboelectric charge density (Adanur, 2000; Chen et al., 2018). This includes increasing the fabric yarn density or stitch density (Huang et al., 2019; Zhang et al., 2016).

Among the methods implemented to enhance electrostatic induction, improving the motion parameters of triboelectric layers has been a key strategy. This includes increasing the motion speed (frequency) of TENG contact surfaces as well as their movement amplitude, which results in increased electrical outputs (Chen et al., 2020, 2018; Xiong et al., 2018). Use of stretchable fabric structures and 3D knitted and woven fabrics such as spacer fabrics showed desirable motion characteristics with good structural integrity and faster recovery. Moreover, the importance of applying adequate contact forces on triboelectric surfaces to enhance the power outputs has been highlighted (Gong et al., 2019a, 2019b). Finally, controlling the thickness of the fabric layers and additional triboelectric material layers has high significance in improving fabric-related TENG outputs (Dong et al., 2017a; Fan et al., 2020; Lee et al., 2015).

## Future Perspectives for Fabric-Based TENG Devices

Early fabric-based TENG developments mainly used woven fabrics, relying on surface modifications via triboelectric coatings (Ko et al., 2015; Lee et al., 2015) and nanostructures (Lee et al., 2015; Seung et al., 2015) to increase electrical outputs, with less attention given to wearable properties. However, with the progress of the technology, it has become increasingly clear that the success of fabric-based TENGs depends on obtaining an acceptable balance between the electrical outputs and wearable properties. More recently, a range of fabric manufacturing methods (knitting, nonwoven, braiding) and surface modification techniques (printing, nanoparticle deposition, fabric pattern variation, grated structures) have

been used, obtaining enhanced wearable properties (air permeability~1068 L/m$^2$, Xiong et al. (2018), and thermal conductivity~8.35 × $10^{-2}$ W/m K, Gong et al. (2019a and 2019b)), less bulk (<0.08 g/cm$^2$ (Gong et al., 2019a, 2019b)), washability, and tactile properties, in addition to improved electrical performances.

Expanding beyond laboratory-scale toward mass-scale production and commercialization, fabric-based TENGs need to be examined in different viewpoints. First, wearable properties of fabric TENGs need to be improved to make them more attractive to the users. Triboelectric modifications typically tend to degrade fabric wearability. Ideally, if textile-based TENG designs can be engineered to comply with the standard performance requirements of commercial textiles, they can be readily integrated into garments without compromising wearable properties. In this regard, fabric weight, fabric strength, air permeability, thermal conductivity, etc., need to be considered. Fabrics are divided into several of weight categories: very lightweight (<1 ounce per square yard (oz Yrd$^2$), lightweight (2–3 oz yrd$^2$), medium weight (5–7 oz yrd$^2$), and heavy weight (>7 oz yrd$^2$) (Li and Dai, 2006), and their applications depend heavily on this categorization (Note S7). Obtaining the desired weight range for a given wearable TENG application is therefore a critical design factor. Fabric strength need to comply with the requirements for specified applications; however, the exact strength specifications vary depending on the apparel manufacturers. Air permeability greatly affects the comfort of a garment, and for a typical textile product, this should be kept between 0.05 and 0.5 m/s to be comfortable for a wearer (Bartels, 2011). The thermal comfort of a fabric depends on its thermal conductivity, which again varies with the end application of the textiles, as summarized in Note S7 (Bartels, 2011). Second, ensuring processability of TENG fabrics using existing textile technologies for dyeing and finishing, etc., will allow their streamlined scaling up. The main parameters affecting this processability include fabric weight and strength, and the TENG fabrics should be designed to comply with these requirements (Hu, 2008). Therefore, in our view, wearability and scalability factors are pivotal in the future success of textile-based TENG technology and should be given careful consideration when designing TENGs.

In a textile engineering perspective, several common fabric manufacturing techniques can potentially be used to develop fabric-based TENGs with enhanced power generation and wearable properties. One of the interesting aspects to consider is the fabric formation methods, which allow precise control of the position, movement, and timing of individual yarns (both width- and lengthwise directions). Such technologies will allow the construction of carefully engineered fabric structures with desired surface textures, porosity, flexible and stretch characteristics, etc., enabling improved electrical and wearable properties for TENGs. Jacquard weaving is one such fabric formation method, which facilitates individual control over each warp and weft yarn of a fabric (Adanur, 2000). Jacquard knitting allows the precise control of each knitted loop by controlling the needle movements and yarn insertion (Spencer, 2001). These jacquard methods provide the potential of constructing TENG architectures with different fabric structures, triboelectric materials, and surface textures, which would enhance triboelectric properties as well as wearable characteristics. Second, the manufacturing techniques that facilitate the construction of multiple fabrics with different materials combined onto a single fabric structure is another useful prospect. These methods include computerized flatbed knitting, 3D knitting (Maziz et al., 2017; Munden, 1959; Spencer, 2001), 3D weaving, and multi-phase weaving (Gandhi and Sondhelm, 2016) techniques, which could allow standalone compact TENG architectures with desirable motion characteristics. Conventionally, TENGs have been incorporated into specified regions of garments, for example, the underarm area (Ning et al., 2018) and the sleeves (Haque et al., 2018), considering the availability of high mechanical power. Instead of traditional integration techniques such as sewing, fabric development methods such as the intarsia knitting technique can be used to incorporate triboelectrically active TENG regions into selected parts of a garment panel with high integrity and seamless finishes (Spencer, 2001), providing the potential to significantly enhance their wearable characteristics.

## TESTING OF TEXTILE-BASED TENGS

Within the brief history of textile-based TENGs, standard techniques to measure their wearable or electrical performances have not yet been established. Herein, we summarize standard test methods used for generic textiles (Note S8) as a guideline for testing wearable properties of textile-based TENGs, along with a summary of electrical characterization methods commonly used for TENGs. Although the type of testing and the threshold evaluation values may vary depending on their end use, examining these test methods could guide the development of future standards for textile-based TENGs.

Considering the wearable characteristics of generic textiles, several test categories including structural, durability, comfort and esthetics, and safety testing can be identified. In addition, a test category termed intelligent testing is being developed to evaluate the performance of smart textiles. These test standards are presented by internationally recognized bodies such as ISO (International Organization for Standardization), BSI (British Standard Institution), ASTM (American Society for Testing and Materials), and AATCC (American Association of Textile Chemists and Colorists) (Hu, 2008). The basic test parameters and the test methods of each of the aforementioned test categories are summarized in Note S8. Designing future textile-based TENGs adhering to these specifications and using the standards as guidelines will ensure that the TENGs contain required wearable properties, which is massively beneficial for their end users.

Textiles should not contain any substances that are harmful to human health such as cytotoxic, irritating, or carcinogenic matter, etc., as they contact human skin and the body. According to REACH (the governing body for European chemical registration, evolution, authorization, and restrictions) there are strict regulations against hazardous substances in textiles, some of which are summarized in Note S9 (Das, 2013). In our view, wearable TENGs should be designed within these guidelines to ensure the safety of the wearers.

Electrical characterization of textile-based TENGs is conducted by different research groups using different methods. These methods include the measurement of current, voltage, charge, and power outputs, using oscilloscopes or electrometers (Dudem et al., 2019; Paosangthong et al., 2019b; Sala de Medeiros et al., 2019; Wang et al., 2020), when the TENG is subjected to mechanical excitation. Mechanical excitation could be provided manually (hand tapping, Lai et al., 2017; Liu et al., 2018a, 2018b; Mallineni et al., 2018; Yang et al., 2018a; bending, Dong et al., 2017a; Zhang et al., 2019, 2016; Zhou et al., 2014a, 2014b) or mechanically (linear motor, Dong et al., 2017b; Zhao et al., 2020), (shaker, Dudem et al., 2020, 2019), with a specified amplitude and speed. In addition, unique analysis techniques such as TENG impedance plots, TENG power transfer equation, and voltage-charge (V-Q) plots are used to investigate TENG outputs. However, the TENG outputs are highly sensitive to number of material, structural, motion, and environmental parameters, as well as to the electrical measurement methods (Dharmasena et al., 2017; Dharmasena et al., 2018a, 2018b; Dharmasena and Silva, 2019a, 2019b). Therefore, output characterization and reporting for textile-based TENGs have often been non-standard, and performance comparison between different devices has not been feasible. This calls for the urgent need to develop standard output characterization methods for TENG devices.

## Summary and Outlook

TENGs are widely regarded as one of the most promising candidates to power the next generation of low-power electronics for mobile, portable, and wearable applications. More recently, significant efforts have been directed toward constructing wearable TENGs to harvest mechanical energy generated through human body movements to power smart textiles, health sensors, etc. To this end, textile technologies provide a wide range of possibilities in constructing highly efficient wearable TENG architectures.

In this work, we presented a comprehensive analysis on the textile-based TENG technology with device optimization and textile engineering perspectives. Following a brief introduction to TENGs, we created a broad platform on TENG output optimization based on our previous theoretical and experimental studies. The technological landscape of textile-based TENGs was discussed in relation to the textile manufacturing process, bridging these apparently distant but closely interrelated technical disciplines. Textile-based TENGs were classified under fiber/yarn- or fabric-based developments, considering the stage at which the triboelectric functionalization takes place in relation to the textile manufacturing process. State-of-the-art developments of each of these TENG categories were highlighted. Subsequently, the progress and optimization techniques used in recent textile-based TENG developments were thoroughly examined.

Within the device optimization criteria, we discussed textile manufacturing methods and processes applicable for the fabrication of TENGs, which contain the potential of enhancing their performances. The success of TENGs in wearable applications depends on the ability to obtain an appropriate balance between their electrical and wearable properties. Herein, we provided insights on the improvement of key textile parameters affecting TENG wearable aspects as well as electrical performances. Scaling up of textile-based TENG technology was a major focus point in this work, and the compatibility of TENG designs

with existing textile machinery and processes was highlighted as the main strategy of achieving this target. To this end, a set of specifications for TENG design parameters were presented as a guideline to ensure this compatibility. Finally, the testing standards potentially applicable for evaluating wearable and electrical properties of textile-based TENGs were summarized. In our view, complying with these test standards and guidelines will be pivotal for successfully fabricating textile-based TENGs, and their scaling up using well-established textile-related technological resources.

Exploring the outlook and prospects of this technology, a number of exciting contemporary trends can be observed. Recent textile-based TENG architectures have produced significantly high electrical output performances (Chen et al., 2020; Gong et al., 2019a, 2019b; Sala de Medeiros et al., 2019) and improved wearable characteristics (Gong et al., 2019a, 2019b; Xiong et al., 2018), which can be attributed to several factors. There were wide expansions in the range of materials used in textile-based TENGs, including conventional and modified textile-related materials (Chen et al., 2018; Choi et al., 2017; Gong et al., 2017; He et al., 2020; Ning et al., 2018; Shi et al., 2016; Song et al., 2017; Yao et al., 2017; Ye et al., 2020a) and conductive polymers (Dudem et al., 2019; Li et al., 2016), etc., along with improved application techniques such as enhanced coating methods (Sala de Medeiros et al., 2019; Zhou et al., 2014a, 2014b) and deposition techniques (Choi et al., 2017; Huang et al., 2019; Paosangthong et al., 2019b; Zhang et al., 2019; Zhou et al., 2014a, 2014b), resulting in improved TENG performances. The structural developments of TENGs have also boosted TENG performances, which were obtained through various micro-fabrication techniques and textile manufacturing methods (e.g., weaving, Chen et al., 2020, 2018; Liu et al., 2020a, 2020b; Lou et al., 2020; Ning et al., 2018; Pu et al., 2016b, 2016a; Shi et al., 2017; knitting, Dong et al., 2017b; Huang et al., 2019; Kwak et al., 2017; nonwoven, Liu et al., 2018a, 2018b; Peng et al., 2019; etc.). More recently, some TENG designs utilized cleverly designed hybridization of several textile manufacturing techniques, which include hybrid knitted/woven (Yi et al., 2019) fabric structures and hybrid yarn/fabric-based structural modifications (Liu et al., 2016), providing enhanced wearable and electrical functionalities compared with conventional devices. Furthermore, textiles have been increasingly used as triboelectric components and active structural elements, providing an escalated degree of device integration.

Developing multi-functional energy harvesting textiles is another notable trend, achieved by hybridizing different technologies. A number of textile-based TENGs were presented, integrating triboelectric energy harvesting and wearable energy storage components, attempting to minimize this issue (Dong et al., 2017b; Pu et al., 2016a, 2015; Song et al., 2017; Wang et al., 2015a, 2015b, 2015c, 2015d; Wen et al., 2016; Yang et al., 2018b). Furthermore, harvesting energy from multiple sources through hybrid triboelectric/piezoelectric (Guo et al., 2018; Kim et al., 2017), triboelectric/solar cell (Chen et al., 2016; Wen et al., 2016), triboelectric/thermoelectric, and triboelectric/solar cell/energy storage (Wen et al., 2016) structures was demonstrated, which would enable self-powered wearable energy systems that efficiently utilize multiple ambient energy sources with a high degree of autonomy. There have been significant improvements in theoretical modeling and optimization methods supported by the DDEF model, TENG impedance plot, V-Q plots, etc., which can be effectively used to further improve the textile-based TENG performances. Furthermore, recent investigations into TENGs have uncovered underlying reasons behind their inherent drawbacks such as the discontinuous and irregular output generation (Dharmasena, 2020), and several innovative methods have been presented such as the development of DC TENG (Dharmasena et al., 2020; Liu et al., 2019a, 2019b) to overcome such issues. These prospects would potentially pave the way toward highly efficient energy harvesting textiles with wearable and durable properties comparable to typical garments in the future.

Several challenges need to be overcome in this technology, to enable sustainable device structures and their scaling up. The electrical output performances of textile-based TENGs still fall behind conventional plastic-based TENG architectures (Dharmasena and Silva, 2019a, 2019b), which need to be improved. This could potentially be achieved by developing triboelectric polymers with stable and high triboelectric charge densities, high conductivity electrodes with wearable and safety characteristics, and highly efficient textile structures, which provide improved friction properties and high-speed movements. Similar strategies could be used to improve wearable characteristics such as comfort properties, durability against the harsh usage conditions of textiles, and safety, which are of equal importance as the electrical properties in a wearable TENG context. Scalability of textile-based TENGs needs to be carefully considered to make them commercially viable. Selecting low-cost, widely available, and recyclable

materials and scalable production methods is important in this regard. Designing TENGs to be compatible with existing textile technologies and standards would also be a critical strategy in overcoming this challenge.

There has not been a standard output characterization for TENGs, making it difficult to evaluate and compare their performances. Due to their high sensitivity to device, motion and environmental parameters, non-linear output generation, and specific measurement requirements, a carefully designed test method needs to be developed for TENGs to obtain reliable and comparable performance data. Moreover, present theoretical methods and optimization techniques that are limited to planar architectures need to be improved to accommodate complex structures and motion characteristics of textile surfaces. In addition, overall improvements are necessary against generic drawbacks of TENG technology such as high impedance and discontinuous outputs, in constructing efficient textile-based TENGs.

In summary, textile-based TENGs have demonstrated remarkable progress, emerging as a prime candidate for powering the next generation of wearable electronics. Developing textile-based TENGs with detailed attention to electrical output performances as well as wearable properties, in synergy with the optimization methods, textile engineering concepts, and manufacturing techniques, will pave the way toward highly efficient sustainable self-powered wearable energy systems.

## Resource Availability

### *Lead Contact*

Further information and requests for resources should be directed to and will be fulfilled by the Lead Contact, R.D. Ishara G. Dharmasena (r.i.dharmasena@lboro.ac.uk).

### *Materials Availability*

Not Applicable.

### *Data and Code Availability*

Not Applicable.

## SUPPLEMENTAL INFORMATION

Supplemental Information can be found online at https://doi.org/10.1016/j.isci.2020.101360.

## ACKNOWLEDGMENTS

K.R.S.D.G. and N.D.W. acknowledge the support from SRC (SRC ST 2019/24) from the University of Moratuwa and the Department Of Textile And Clothing Technology for funding this research work. K.R.S.D.G. acknowledges the discussions on textile testing with Mr. S.N. Niles of the Department of Textile and Clothing Technology, University of Moratuwa. R.D.I.G.D. acknowledges the support of the Doctoral Prize Fellowship from Loughborough University, for funding this work. This work was also supported by the UK EPSRC Joint University Industry Consortium for Energy (Materials) and Devices Hub (JUICED Hub) (EP/R023662/1). R.D.I.G.D. is grateful to Professor Upul Wijayantha (Loughborough University principle investigator of the JUICED Hub) for discussions about the manuscript.

## AUTHOR CONTRIBUTIONS

R.D.I.G.D and K.R.S.D.G. conceived the idea designed the structure. R.D.I.G.D. and N.D.W. supervised the project. K.R.S.D.G. and N.D.W. wrote the first draft of the manuscript. All authors commented, edited, and revised the final manuscript.

## REFERENCES

Acar, M., Bilgin, S., Versteeg, H.K., Dani, N., and Oxenham, W. (2006). The mechanism of the air-jet texturing: the role of wetting, spin finish and friction in forming and fixing loops. Text. Res. J. *76*, 116–125.

Adanur, S. (2000). Handbook of Weaving, 1st ed (CRC Press).

Ahmad, S., Rasheed, A., Afzal, A., and Ahmad, F. (2017). Advanced Textile Testing Techniques, Advanced Textile Testing Techniques (CRC Press).

Ahn, Y., Song, S., and Yun, K.S. (2015). Woven flexible textile structure for wearable power-generating tactile sensor array. Smart Mater. Struct. *24*, 75002.

Asghar, A., Ahmad, M.R., Yahya, M.F., Hassan, S.Z.U., and Kashif, M. (2019). Hybrid cover yarn's element orientation and its impacts on mechanical/tensile behavior of conductive yarns and fabrics. In Functional Textiles and

Clothing, A. Majumdar, ed. (Springer Singapore), pp. 77–90.

Bai, Z., Zhang, Z., Li, J., and Guo, J. (2019). Textile-based triboelectric nanogenerators with high-performance via optimized functional elastomer composited tribomaterials as wearable power source. Nano Energy *65*, 104012.

Bartels, V.T. (2011). Improving comfort in sports and leisure wear. In Improving Comfort in Clothing, G. Song, ed. (Elsevier Ltd.), pp. 385–411.

Baytekin, H.T., Patashinski, A.Z., Branicki, M., Baytekin, B., Soh, S., and Grzybowski, B.A. (2011a). The mosaic of surface charge in contact electrification. Science *333*, 308–312.

Baytekin, H.T., Patashinski, A.Z., Branicki, M., Baytekin, B., Soh, S., and Grzybowski, B.A. (2011b). The mosaic of surface charge in contact electrification. Science *333*, 308–312.

Baytekin, H.T., Baytekin, B., Incorvati, J.T., and Grzybowski, B.A. (2012). Material transfer and polarity reversal in contact charging. Angew. Chem. *124*, 4927–4931.

Byun, K.E., Lee, M.H., Cho, Y., Nam, S.G., Shin, H.J., and Park, S. (2017). Potential role of motion for enhancing maximum output energy of triboelectric nanogenerator. APL Mater. *5*, 074107.

Cayuela, D., Montero, L., Díaz, J., Algaba, I., and Manich, A.M. (2012). Microstructure variations of polylactide fibres with texturing conditions. Text. Res. J. *82*, 1996–2005.

Chai, Z., Zhang, N., Sun, P., Huang, Y., Zhao, C., Fan, H.J., Fan, X., and Mai, W. (2016). Tailorable and wearable textile devices for solar energy harvesting and simultaneous storage. ACS Nano *10*, 9201–9207.

Chen, J., Huang, Y., Zhang, N., Zou, H., Liu, R., Tao, C., Fan, X., and Wang, Z.L. (2016). Micro-cable structured textile for simultaneously harvesting solar and mechanical energy. Nat. Energy *1*, 16138.

Chen, J., Guo, H., Pu, X., Wang, X., Xi, Y., and Hu, C. (2018). Traditional weaving craft for one-piece self-charging power textile for wearable electronics. Nano Energy *50*, 536–543.

Chen, C., Guo, H., Chen, L., Wang, Y.-C., Pu, X., Yu, W., Wang, F., Du, Z., and Wang, Z.L. (2020). Direct current fabric triboelectric nanogenerator for biomotion energy harvesting. ACS Nano *14*, 4585–4594.

Cheng, Y., Lu, X., Hoe Chan, K., Wang, R., Cao, Z., Sun, J., and Wei Ho, G. (2017). A stretchable fiber nanogenerator for versatile mechanical energy harvesting and self-powered full-range personal healthcare monitoring. Nano Energy *41*, 511–518.

Cheon, S., Kang, H., Kim, H., Son, Y., Lee, J.Y., Shin, H.-J., Kim, S.-W., and Cho, J.H. (2018). High-performance triboelectric nanogenerators based on electrospun polyvinylidene fluoride-silver nanowire composite nanofibers. Adv. Funct. Mater. *28*, 1703778.

Choi, Y.J., and Kim, S.H. (2015). Characterization of recycled polyethylene terephthalates and polyethylene terephthalate–nylon6 blend knitted fabrics. Text. Res. J. *85*, 337–345.

Choi, A.Y., Lee, C.J., Park, J., Kim, D., and Kim, Y.T. (2017). Corrugated textile based triboelectric generator for wearable energy harvesting. Sci. Rep. *7*, 7–12.

Das, S. (2013). Product safety and restricted substances in apparel. In Product Safety and Restricted Substances in Apparel, 2nd ed, S. Das, ed. (WPI Publishing).

Deane, J.H.B., Dharmasena, R.D.I.G., and Gentile, G. (2018). Power computation for the triboelectric nanogenerator. Nano Energy *54*, 39–49.

Dharmasena, R.D.I.G. (2019). Triboelectric Self-Powered Energy Systems (University of Surrey).

Dharmasena, R.D.I.G. (2020). Inherent asymmetry of the current output in a triboelectric nanogenerator. Nano Energy *76*, 105045.

Dharmasena, R.D.I.G., and Silva, S.R.P. (2019a). Towards optimized triboelectric nanogenerators. Nano Energy *62*, 530–549.

Dharmasena R.D.I.G., Silva, S.R.P., 2019b. Triboelectric Generator. United Kingdom Patent Application No. GB2019/053344.

Dharmasena, R.D.I.G., Jayawardena, K.D.G.I., Mills, C.A., Deane, J.H.B., Anguita, J.V., Dorey, R.A., and Silva, S.R.P. (2017). Triboelectric nanogenerators: providing a fundamental framework. Energy Environ. Sci. *10*, 1801–1811.

Dharmasena, R.D.I.G., Jayawardena, K.D.G.I., Mills, C.A., Dorey, R.A., and Silva, S.R.P. (2018a). A unified theoretical model for Triboelectric Nanogenerators. Nano Energy *48*, 391–400.

Dharmasena, R.D.I.G., Deane, J.H.B., and Silva, S.R.P. (2018b). Nature of power generation and output optimization criteria for triboelectric nanogenerators. Adv. Energy Mater. *8*, 1–11.

Dharmasena, R.D.I.G., Jayawardena, K.D.G.I., Saadi, Z., Yao, X., Bandara, R.M.I., Zhao, Y., and Silva, S.R.P. (2019). Energy scavenging and powering E-skin functional devices. Proc. IEEE *107*, 2118–2136.

Dharmasena, R.D.I.G., Cronin, H.M., Dorey, R.A., and Silva, S.R.P. (2020). Direct current contact-mode triboelectric nanogenerators via systematic phase shifting. Nano Energy *75*, 104887.

Diaz, A.F., and Felix-Navarro, R.M. (2004). A semi-quantitative tribo-electric series for polymeric materials: the influence of chemical structure and properties. J. Electrostat. *62*, 277–290.

Ding, W., Wang, A.C., Wu, C., Guo, H., and Wang, Z.L. (2019). Human–machine interfacing enabled by triboelectric nanogenerators and tribotronics. Adv. Mater. Technol. *4*, 1800487.

Dong, K., Deng, J., Zi, Y., Wang, Y.C., Xu, C., Zou, H., Ding, W., Dai, Y., Gu, B., Sun, B., and Wang, Z.L. (2017a). 3D orthogonal woven triboelectric nanogenerator for effective biomechanical energy harvesting and as self-powered active motion sensors. Adv. Mater. *29*, 1–11.

Dong, K., Wang, Y.C., Deng, J., Dai, Y., Zhang, S.L., Zou, H., Gu, B., Sun, B., and Wang, Z.L. (2017b). A highly stretchable and washable all-yarn-based self-charging knitting power textile composed of fiber triboelectric nanogenerators and supercapacitors. ACS Nano *11*, 9490–9499.

Dong, K., Wu, Z., Deng, J., Wang, A.C., Zou, H., Chen, C., Hu, D., Gu, B., Sun, B., and Wang, Z.L. (2018). A stretchable yarn embedded triboelectric nanogenerator as electronic skin for biomechanical energy harvesting and multifunctional pressure sensing. Adv. Mater. *30*, 1–12.

Dudem, B., Mule, A.R., Patnam, H.R., and Yu, J.S. (2019). Wearable and durable triboelectric nanogenerators via polyaniline coated cotton textiles as a movement sensor and self-powered system. Nano Energy *55*, 305–315.

Dudem, B., Dharmasena, R.D.I.G., Graham, S.A., Leem, J.W., Patnam, H., Mule, A.R., Silva, S.R.P., and Yu, J.S. (2020). Exploring theoretical and experimental optimization towards high-performance triboelectric nanogenerators using microarchitecture silk cocoon films. Nano Energy, 104882, https://doi.org/10.1016/j.nanoen.2020.104882.

Eichhorn, S.J., Hearle, J.W.S., Jaffe, M., and Kikutani, T. (2009). Handbook of Textile Fibre Structure, Handbook of Textile Fibre Structure (Elsevier Inc).

Fan, F.R., Tian, Z.Q., and Lin Wang, Z. (2012). Flexible triboelectric generator. Nano Energy *1*, 328–334.

Fan, K., Liu, Z., Liu, H., Wang, L., Zhu, Y., and Yu, B. (2017). Scavenging energy from human walking through a shoe-mounted piezoelectric harvester. Appl. Phys. Lett. *110*, 143902.

Fan, W., He, Q., Meng, K., Tan, X., Zhou, Z., Zhang, G., Yang, J., and Wang, Z.L. (2020). Machine-knitted washable sensor array textile for precise epidermal physiological signal monitoring. Sci. Adv. *6*, eaay2840.

Fernando, E.A.S.K., Dharmasena, I.G., and Niles, S.N. (2017). Kaolin shear thickening fluid reinforced uhmwpe composites for protective clothing. Indian J. Fibre Text. Res. *42*, 241–244.

Foster, E.J., Moon, R.J., Agarwal, U.P., Bortner, M.J., Bras, J., Camarero-Espinosa, S., Chan, K.J., Clift, M.J.D., Cranston, E.D., Eichhorn, S.J., et al. (2018). Current characterization methods for cellulose nanomaterials. Chem. Soc. Rev. https://doi.org/10.1039/c6cs00895j.

Galembeck, F., Burgo, T.A.L., Balestrin, L.B.S., Gouveia, R.F., Silva, C.A., and Galembeck, A. (2014). Friction, tribochemistry and triboelectricity: recent progress and perspectives. RSC Adv. https://doi.org/10.1039/c4ra09604e.

Gandhi, K.L., and Sondhelm, W.S. (2016). Technical fabric structures – 1. Woven fabrics. In Handbook of Technical Textiles, A.R. Horrocks and S.C. Anand, eds. (Elsevier), pp. 63–106.

George, H.H. (1982). Model of steady-state melt spinning at intermediate take-up speeds. Polym. Eng. Sci. *22*, 292–299.

Gong, W., Hou, C., Guo, Y., Zhou, J., Mu, J., Li, Y., Zhang, Q., and Wang, H. (2017). A wearable, fibroid, self-powered active kinematic sensor

based on stretchable sheath-core structural triboelectric fibers. Nano Energy *39*, 673–683.

Gong, J., Xu, B., Guan, X., Chen, Y., Li, S., and Feng, J. (2019a). Towards truly wearable energy harvesters with full structural integrity of fiber materials. Nano Energy *58*, 365–374.

Gong, W., Hou, C., Zhou, J., Guo, Y., Zhang, W., Li, Y., Zhang, Q., and Wang, H. (2019b). Continuous and scalable manufacture of amphibious energy yarns and textiles. Nat. Commun. *10*, 868.

Guo, Y., Zhang, X.S., Wang, Y., Gong, W., Zhang, Q., Wang, H., and Brugger, J. (2018). All-fiber hybrid piezoelectric-enhanced triboelectric nanogenerator for wearable gesture monitoring. Nano Energy *48*, 152–160.

Guo, Y., Cao, Y., Chen, Z., Li, R., Gong, W., Yang, W., Zhang, Q., and Wang, H. (2020). Fluorinated metal-organic framework as bifunctional filler toward highly improving output performance of triboelectric nanogenerators. Nano Energy *70*, 104517.

Ha, M., Park, J., Lee, Y., and Ko, H. (2015). Triboelectric generators and sensors for self-powered wearable electronics. ACS Nano *9*, 3421–3427.

Haque, R.I., Farine, P.-A., and Briand, D. (2018). Soft triboelectric generators by use of cost-effective elastomers and simple casting process. Sens. Actuat. A Phys. *271*, 88–95.

Harvey, C., Holtzman, E., Ko, J., Hagan, B., Wu, R., Marschner, S., and Kessler, D. (2019). Weaving objects: spatial design and functionality of 3D-woven textiles. Leonardo *52*, 381–388.

He, X., Zi, Y., Guo, H., Zheng, H., Xi, Y., Wu, C., Wang, J., Zhang, W., Lu, C., and Wang, Z.L. (2017). A highly stretchable fiber-based triboelectric nanogenerator for self-powered wearable electronics. Adv. Funct. Mater. *27*, 1–8.

He, Q., Wu, Y., Feng, Z., Fan, W., Lin, Z., Sun, C., Zhou, Z., Meng, K., Wu, W., and Yang, J. (2019). An all-textile triboelectric sensor for wearable teleoperated human–machine interaction. J. Mater. Chem. A *7*, 26804–26811.

He, F., You, X., Gong, H., Yang, Y., Bai, T., Wang, W., Guo, W., Liu, X., and Ye, M. (2020). Stretchable, biocompatible, and multifunctional silk fibroin-based hydrogels toward wearable strain/pressure sensors and triboelectric nanogenerators. ACS Appl. Mater. Interfaces *12*, 6442–6450.

Hu, J. (2008). Fabric Testing, Fabric Testing (Woodhead Publishing Limited).

Huang, T., Zhang, J., Yu, B., Yu, H., Long, H., Wang, H., Zhang, Q., and Zhu, M. (2019). Fabric texture design for boosting the performance of a knitted washable textile triboelectric nanogenerator as wearable power. Nano Energy *58*, 375–383.

Invernizzi, F., Dulio, S., Patrini, M., Guizzetti, G., and Mustarelli, P. (2016). Energy harvesting from human motion: materials and techniques. Chem. Soc. Rev. https://doi.org/10.1039/c5cs00812c.

Jung, S., Hong, S., Kim, J., Lee, S., Hyeon, T., Lee, M., and Kim, D.-H. (2015). Wearable fall detector using integrated sensors and energy devices. Sci. Rep. *5*, 17081.

Kim, K., Song, G., Park, C., and Yun, K.-S. (2017). Multifunctional woven structure operating as triboelectric energy harvester, capacitive tactile sensor array, and piezoresistive strain sensor array. Sensors *17*, 2582.

Kim, D., Park, J., and Kim, Y.T. (2019). Core-shell and helical-structured cylindrical triboelectric nanogenerator for wearable energy harvesting. ACS Appl. Energy Mater. *2*, 1357–1362.

Kim, J., Kim, W., Jang, G., Hyeon, D.S., Park, M.H., and Hong, J.P. (2020). 1D stretchable block copolymer yarn-based energy harvesters via BaTiO 3/polydimethylsiloxane composite-carbon conductive ink. Adv. Energy Mater. *10*, 1903217.

Ko, Y.H., Nagaraju, G., and Yu, J.S. (2015). Multi-stacked PDMS-based triboelectric generators with conductive textile for efficient energy harvesting. RSC Adv. *5*, 6437–6442.

Koo, H.R., Lee, Y.J., Gi, S., Khang, S., Lee, J.H., Lee, J.H., Lim, M.G., Park, H.J., and Lee, J.W. (2014). The effect of textile-based inductive coil sensor positions for heart rate monitoring. J. Med. Syst. *38*, https://doi.org/10.1007/s10916-013-0002-0.

Kwak, S.S., Kim, H., Seung, W., Kim, J., Hinchet, R., and Kim, S.-W. (2017). Fully stretchable textile triboelectric nanogenerator with knitted fabric structures. ACS Nano *11*, 10733–10741.

Lai, Y.-C., Deng, J., Zhang, S.L., Niu, S., Guo, H., and Wang, Z.L. (2017). Single-thread-based wearable and highly stretchable triboelectric nanogenerators and their applications in cloth-based self-powered human-interactive and biomedical sensing. Adv. Funct. Mater. *27*, 1604462.

Lawrence, C.A. (2010). Advances in Yarn Spinning Technology, Advances in Yarn Spinning Technology (Woodhead Publishing).

Lee, M.E.M., and Ockendon, H. (2006). The transfer of fibres in the carding machine. J. Eng. Math. *54*, 261–271.

Lee, S., Ko, W., Oh, Y., Lee, J., Baek, G., Lee, Y., Sohn, J., Cha, S., Kim, J., Park, J., and Hong, J. (2015). Triboelectric energy harvester based on wearable textile platforms employing various surface morphologies. Nano Energy *12*, 410–418.

Li, Y., and Dai, X.Q. (2006). Biomechanical Engineering of Textiles and Clothing. In Biomechanical Engineering of Textiles and Clothing, 1st ed, Y. Li and X.Q. Dai, eds. (Woodhead Publishing).

Li, Z., Ma, G., Ge, R., Qin, F., Dong, X., Meng, W., Liu, T., Tong, J., Jiang, F., Zhou, Y., et al. (2016). Free-standing conducting polymer films for high-performance energy devices. Angew. Chem. Int. Ed. *55*, 979–982.

Li, Z., Zhu, M., Shen, J., Qiu, Q., Yu, J., and Ding, B. (2020). All-fiber structured electronic skin with high elasticity and breathability. Adv. Funct. Mater. *30*, 1908411.

Liu, C., and Bard, A.J. (2008). Electrostatic electrochemistry at insulators. Nat. Mater. *7*, 505–509.

Liu, L., Pan, J., Chen, P., Zhang, J., Yu, X., Ding, X., Wang, B., Sun, X., and Peng, H. (2016). A triboelectric textile templated by a three-dimensionally penetrated fabric. J. Mater. Chem. A *4*, 6077–6083.

Liu, G., Nie, J., Han, C., Jiang, T., Yang, Z., Pang, Y., Xu, L., Guo, T., Bu, T., Zhang, C., and Wang, Z.L. (2018a). Self-powered electrostatic adsorption face mask based on a triboelectric nanogenerator. ACS Appl. Mater. Interfaces *10*, 7126–7133.

Liu, S., Zheng, W., Yang, B., and Tao, X. (2018b). Triboelectric charge density of porous and deformable fabrics made from polymer fibers. Nano Energy *53*, 383–390.

Liu, D., Yin, X., Guo, H., Zhou, L., Li, X., Zhang, C., Wang, J., and Wang, Z.L. (2019a). A constant current triboelectric nanogenerator arising from electrostatic breakdown. Sci. Adv. *5*, eaav6437.

Liu, J., Gu, L., Cui, N., Bai, S., Liu, S., Xu, Q., Qin, Y., Yang, R., and Zhou, F. (2019b). Core-shell fiber-based 2D woven triboelectric nanogenerator for effective motion energy harvesting. Nanoscale Res. Lett. *14*, 311.

Liu, H., Wang, H., Lyu, Y., He, C., and Liu, Z. (2020a). A novel triboelectric nanogenerator based on carbon fiber reinforced composite lamina and as a self-powered displacement sensor. Microelectron. Eng. *224*, 111231.

Liu, L., Yang, X., Zhao, L., Xu, W., Wang, J., Yang, Q., and Tang, Q. (2020b). Nanowrinkle-patterned flexible woven triboelectric nanogenerator toward self-powered wearable electronics. Nano Energy *73*, 104797.

Lou, M., Abdalla, I., Zhu, M., Wei, X., Yu, J., Li, Z., and Ding, B. (2020). Highly wearable, breathable, and washable sensing textile for human motion and pulse monitoring. ACS Appl. Mater. Interfaces *12*, 19965–19973.

Ma, L., Zhou, M., Wu, R., Patil, A., Gong, H., Zhu, S., Wang, T., Zhang, Y., Shen, S., Dong, K., et al. (2020). Continuous and scalable manufacture of hybridized nano-micro triboelectric yarns for energy harvesting and signal sensing. ACS Nano *14*, 4716–4726.

Mallineni, S.S.K., Dong, Y., Behlow, H., Rao, A.M., and Podila, R. (2018). A wireless triboelectric nanogenerator. Adv. Energy Mater. *8*, 1702736.

Manero, R.B.R., Shafti, A., Michael, B., Grewal, J., Fernandez, J.L.R., Althoefer, K., and Howard, M.J. (2016). Wearable embroidered muscle activity sensing device for the human upper leg. In Proceedings of the Annual International Conference of the IEEE Engineering in Medicine and Biology Society, J. Patton, ed. (EMBS. Institute of Electrical and Electronics Engineers Inc.), pp. 6062–6065.

Matsunaga, M., Hirotani, J., Kishimoto, S., and Ohno, Y. (2020). High-output, transparent, stretchable triboelectric nanogenerator based on carbon nanotube thin film toward wearable energy harvesters. Nano Energy *67*, 104297.

Maziz, A., Concas, A., Khaldi, A., Stålhand, J., Persson, N.-K., and Jager, E.W.H. (2017). Knitting and weaving artificial muscles. Sci. Adv. *3*, e1600327.

McCarty, L.S., and Whitesides, G.M. (2008). Electrostatic charging due to separation of ions at interfaces: contact electrification of ionic electrets. Angew. Chem. Int. Ed. *47*, 2188–2207.

McIntyre, J.E. (2005). Synthetic Fibres, 1st ed. (Woodhead Publishing).

McIntyre, J.E., and Daniels, P.N. (1995). Textile Terms and Definitions (Taylor & Francis).

Munden, D.L. (1959). 26—the geometry and dimensional properties OF plain-knit fabrics. J. Text. Inst. Trans. *50*, T448–T471.

Nair, G.P. (2011). Methods and Machinery for the Dyeing process, Handbook of Textile and Industrial Dyeing: Principles, Processes and Types of Dyes (Woodhead Publishing Limited).

Ning, C., Tian, L., Zhao, X., Xiang, S., Tang, Y., Liang, E., and Mao, Y. (2018). Washable textile-structured single-electrode triboelectric nanogenerator for self-powered wearable electronics. J. Mater. Chem. A *6*, 19143–19150.

Niu, S., Wang, S., Lin, L., Liu, Y., Zhou, Y.S., Hu, Y., and Wang, Z.L. (2013). Theoretical study of contact-mode triboelectric nanogenerators as an effective power source. Energy Environ. Sci. *6*, 3576–3583.

Pan, R., Xuan, W., Chen, J., Dong, S., Jin, H., Wang, X., Li, H., and Luo, J. (2018). Fully biodegradable triboelectric nanogenerators based on electrospun polylactic acid and nanostructured gelatin films. Nano Energy *45*, 193–202.

Paosangthong, W., Torah, R., and Beeby, S. (2019a). Recent progress on textile-based triboelectric nanogenerators. Nano Energy *55*, 401–423.

Paosangthong, W., Wagih, M., Torah, R., and Beeby, S. (2019b). Textile-based triboelectric nanogenerator with alternating positive and negative freestanding grating structure. Nano Energy *66*, 104148.

Park, J., Choi, A.Y., Lee, C.J., Kim, D., and Kim, Y.T. (2017). Highly stretchable fiber-based single-electrode triboelectric nanogenerator for wearable devices. RSC Adv. *7*, 54829–54834.

Park, J., Kim, D., Kim, Y.T., 2018. Flexible fiber based woven structured triboelectric nanogenerator for self-powered system, in: 2018 IEEE 18th International Conference on Nanotechnology (IEEE-NANO). IEEE, pp. 1–4.

De Pauw, B., Berghmans, F., Thienpont, H., Verdiere, P., and Geernaert, T. (2020). Optical fiber-based sensors as an experimental tool to assess the weft and warp yarn tension beam-to-roll in rapier weaving machines. Text. Res. J. *90*, 857–865.

Peng, F., Liu, D., Zhao, W., Zheng, G., Ji, Y., Dai, K., Mi, L., Zhang, D., Liu, C., and Shen, C. (2019). Facile fabrication of triboelectric nanogenerator based on low-cost thermoplastic polymeric fabrics for large-area energy harvesting and self-powered sensing. Nano Energy *65*, 104068.

Petrulis, D., and Petrulyte, S. (2009). Effect of manufacturing parameters of covered yarns on the geometry of covering components. Text. Res. J. *79*, 526–533.

Pu, X., Li, L., Song, H., Du, C., Zhao, Z., Jiang, C., Cao, G., Hu, W., and Wang, Z.L. (2015). A self-charging power unit by integration of a textile triboelectric nanogenerator and a flexible lithium-ion battery for wearable electronics. Adv. Mater. *27*, 2472–2478.

Pu, X., Li, L., Liu, M., Jiang, C., Du, C., Zhao, Z., Hu, W., and Wang, Z.L. (2016a). Wearable self-charging power textile based on flexible yarn supercapacitors and fabric nanogenerators. Adv. Mater. *28*, 98–105.

Pu, X., Song, W., Liu, M., Sun, C., Du, C., Jiang, C., Huang, X., Zou, D., Hu, W., and Wang, Z.L. (2016b). Wearable power-textiles by integrating fabric triboelectric nanogenerators and fiber-shaped dye-sensitized solar cells. Adv. Energy Mater. *6*, 1601048.

Riemer, R., and Shapiro, A. (2011). Biomechanical energy harvesting from human motion: theory, state of the art, design guidelines, and future directions. J. Neuroeng. Rehabil. *8*, https://doi.org/10.1186/1743-0003-8-22.

Russell, S.J. (2007). Handbook of Nonwovens, Handbook of Nonwovens (Woodhead Publishing Limited).

Sala de Medeiros, M., Chanci, D., Moreno, C., Goswami, D., and Martinez, R.V. (2019). Waterproof, breathable, and antibacterial self-powered e-textiles based on omniphobic triboelectric nanogenerators. Adv. Funct. Mater. *29*, 1904350.

Schegner, P., Fazeli, M., Sennewald, C., Hoffmann, G., and Cherif, C. (2019). Technology development for direct weaving of complex 3D nodal structures. Appl. Compos. Mater. *26*, 423–432.

Sengupta, A.K., Kothari, V.K., and Sensarma, J.K. (1995). Mechanism of nep formation in air-jet texturing. Text. Res. J. *65*, 273–277.

Seung, W., Gupta, M.K., Lee, K.Y., Shin, K.S., Lee, J.H., Kim, T.Y., Kim, S., Lin, J., Kim, J.H., and Kim, S.W. (2015). Nanopatterned textile-based wearable triboelectric nanogenerator. ACS Nano *9*, 3501–3509.

Shi, M., Wu, H., Zhang, J., Han, M., Meng, B., and Zhang, H. (2017). Self-powered wireless smart patch for healthcare monitoring. Nano Energy *32*, 479–487.

Sim, H.J., Choi, C., Kim, S.H., Kim, K.M., Lee, C.J., Kim, Y.T., Lepró, X., Baughman, R.H., and Kim, S.J. (2016). Stretchable triboelectric fiber for self-powered kinematic sensing textile. Sci. Rep. *6*, 35153.

Somkuwar, V.U., Pragya, A., and Kumar, B. (2020). Structurally engineered textile-based triboelectric nanogenerator for energy harvesting application. J. Mater. Sci. *55*, 5177–5189.

Song, Y., Zhang, J., Guo, H., Chen, X., Su, Z., Chen, H., Cheng, X., and Zhang, H. (2017). All-fabric-based wearable self-charging power cloth. Appl. Phys. Lett. *111*, 073901.

Spencer, D.J. (2001). Knitting Technology : A Comprehensive Handbook and Practical Guide, 1st ed. (CRC Press).

Stoppa, M., and Chiolerio, A. (2014). Wearable electronics and smart textiles: a critical review. Sensors *14*, 11957–11992.

Tian, Z., He, J., Chen, X., Zhang, Z., Wen, T., Zhai, C., Han, J., Mu, J., Hou, X., Chou, X., and Xue, C. (2017). Performance-boosted triboelectric textile for harvesting human motion energy. Nano Energy *39*, 562–570.

Tian, Z., He, J., Chen, X., Wen, T., Zhai, C., Zhang, Z., Cho, J., Chou, X., and Xue, C. (2018). Core–shell coaxially structured triboelectric nanogenerator for energy harvesting and motion sensing. RSC Adv. *8*, 2950–2957.

Todor, M.P., Bulei, C., Heput, T., and Kiss, I. (2018). Researches on the development of new composite materials complete/partially biodegradable using natural textile fibers of new vegetable origin and those recovered from textile waste. IOP Conf. Ser. Mater. Sci. Eng. *294*, https://doi.org/10.1088/1757-899X/294/1/012021.

Wanasekara, N.D., and Eichhorn, S.J. (2017). Injectable highly loaded cellulose nanocrystal fibers and composites. ACS Macro Lett. *6*, 1066–1070.

Wanasekara, N.D., Michud, A., Zhu, C., Rahatekar, S., Sixta, H., and Eichhorn, S.J. (2016). Deformation mechanisms in ionic liquid spun cellulose fibers. Polymer *99*, 222–230.

Wanasekara, N.D., Stone, D.A., Wnek, G.E., and Korley, L.T.J. (2012). Stimuli-responsive and mechanically-switchable electrospun composites. Macromolecules *45*, 9092–9099.

Wang, Z.L. (2017). On Maxwell's displacement current for energy and sensors: the origin of nanogenerators. Mater. Today *20*, 74–82.

Wang, J., Li, X., Zi, Y., Wang, S., Li, Z., Zheng, L., Yi, F., Li, S., and Wang, Z.L. (2015a). A flexible fiber-based supercapacitor-triboelectric-nanogenerator power system for wearable electronics. Adv. Mater. *27*, 4830–4836.

Wang, S., Lin, L., and Wang, Z.L. (2015b). Triboelectric nanogenerators as self-powered active sensors. Nano Energy *11*, 436–462.

Wang, X., Dong, L., Zhang, H., Yu, R., Pan, C., and Wang, Z.L. (2015c). Recent progress in electronic skin. Adv. Sci. *2*, 1–21.

Wang, Z.L., Chen, J., and Lin, L. (2015d). Progress in triboelectric nanogenerators as a new energy technology and self-powered sensors. Energy Environ. Sci. *8*, 2250–2282.

Wang, Y., Xu, Y., Wang, D., Zhang, Y., Zhang, X., Liu, J., Zhao, Y., Huang, C., and Jin, X. (2019). Polytetrafluoroethylene/polyphenylene sulfide needle-punched triboelectric air filter for efficient particulate matter removal. ACS Appl. Mater. Interfaces *11*, 48437–48449.

Wang, W., Yu, A., Liu, X., Liu, Y., Zhang, Y., Zhu, Y., Lei, Y., Jia, M., Zhai, J., and Wang, Z.L. (2020). Large-scale fabrication of robust textile triboelectric nanogenerators. Nano Energy *71*, 104605.

Wardman, R.H. (2017). An Introduction to Textile Coloration, an Introduction to Textile Coloration (John Wiley & Sons, Ltd).

Wen, Z., Yeh, M.-H., Guo, H., Wang, J., Zi, Y., Xu, W., Deng, J., Zhu, L., Wang, X., Hu, C., et al. (2016). Self-powered textile for wearable electronics by hybridizing fiber-shaped nanogenerators, solar cells, and supercapacitors. Sci. Adv. *2*, e1600097.

Weng, W., Chen, P., He, S., Sun, X., and Peng, H. (2016). Smart electronic textiles. Angew. Chem. Int. Ed. *55*, 6140–6169.

R.N. Wijesena, Tissera, P.N.D., de Silva, K.M.N., Amaratunga, G.A.J., Dharmasena, R.D.I.G., Bandara, W.R.L.N., Wijenayaka, A.K.L.A., Bandara, R.M.I., 2016. Near Infrared Energy Absorbing Textile. US20170314185A1.

Wu, C., Wang, A.C., Ding, W., Guo, H., and Wang, Z.L. (2019). Triboelectric nanogenerator: a foundation of the energy for the new era. Adv. Energy Mater. *9*, 1–25.

Xiong, J., Cui, P., Chen, X., Wang, J., Parida, K., Lin, M.F., and Lee, P.S. (2018). Skin-touch-actuated textile-based triboelectric nanogenerator with black phosphorus for durable biomechanical energy harvesting. Nat. Commun. *9*, 1–9.

Xu, C., Zi, Y., Wang, A.C., Zou, H., Dai, Y., He, X., Wang, P., Wang, Y.C., Feng, P., Li, D., and Wang, Z.L. (2018). On the electron-transfer mechanism in the contact-electrification effect. Adv. Mater. *30*, 1–9.

Yang, Y., Sun, N., Wen, Z., Cheng, P., Zheng, H., Shao, H., Xia, Y., Chen, C., Lan, H., Xie, X., et al. (2018a). Liquid-metal-based super-stretchable and structure-designable triboelectric nanogenerator for wearable electronics. ACS Nano *12*, 2027–2034.

Yang, Y., Xie, L., Wen, Z., Chen, C., Chen, X., Wei, A., Cheng, P., Xie, X., and Sun, X. (2018b). Coaxial triboelectric nanogenerator and supercapacitor fiber-based self-charging power fabric. ACS Appl. Mater. Interfaces *10*, 42356–42362.

Yao, C., Yin, X., Yu, Y., Cai, Z., and Wang, X. (2017). Chemically functionalized natural cellulose materials for effective triboelectric nanogenerator development. Adv. Funct. Mater. *27*, 1700794.

Ye, C., Dong, S., Ren, J., and Ling, S. (2020a). Ultrastable and high-performance silk energy harvesting textiles. Nano Micro Lett. *12*, 1–15.

Ye, C., Xu, Q., Ren, J., and Ling, S. (2020b). Violin string inspired core-sheath silk/steel yarns for wearable triboelectric nanogenerator applications. Adv. Fiber Mater. *2*, 24–33.

Yetisen, A.K., Qu, H., Manbachi, A., Butt, H., Dokmeci, M.R., Hinestroza, J.P., Skorobogatiy, M., Khademhosseini, A., and Yun, S.H. (2016). Nanotechnology in textiles. ACS Nano *10*, 3042–3068.

Yi, Z., Ali, M., Gong, X., Dai, H., and Zhongmin, D. (2019). An experimental investigation of the yarn pull-out behavior of plain weave with leno and knitted insertions. Text. Res. J. *89*, 4717–4731.

Yoshimura, G.-I., Iwaki, N., Shintaku, S., and Takayama, T. (1969). The mechanical properties of the covered yarn. J. Text. Mach. Soc. Jpn. *22*, T232–T242.

Yu, A., Pu, X., Wen, R., Liu, M., Zhou, T., Zhang, K., Zhang, Y., Zhai, J., Hu, W., and Wang, Z.L. (2017). Core–shell-yarn-based triboelectric nanogenerator textiles as power cloths. ACS Nano *11*, 12764–12771.

Zhang, D. (2014). Advances in filament yarn spinning of textiles and polymers. In Advances in Filament Yarn Spinning of Textiles and Polymers, 1st ed, D. Zhang, ed. (WOODHEAD).

Zhang, L., Yu, Y., Eyer, G.P., Suo, G., Kozik, L.A., Fairbanks, M., Wang, X., and Andrew, T.L. (2016). All-textile triboelectric generator compatible with traditional textile process. Adv. Mater. Technol. *1*, 1600147.

Zhang, X.S., Han, M., Kim, B., Bao, J.F., Brugger, J., and Zhang, H. (2018). All-in-one self-powered flexible microsystems based on triboelectric nanogenerators. Nano Energy. https://doi.org/10.1016/j.nanoen.2018.02.046.

Zhang, L., Su, C., Cheng, L., Cui, N., Gu, L., Qin, Y., Yang, R., and Zhou, F. (2019). Enhancing the performance of textile triboelectric nanogenerators with oblique microrod arrays for wearable energy harvesting. ACS Appl. Mater. Interfaces *11*, 26824–26829.

Zhao, Z., Pu, X., Du, C., Li, L., Jiang, C., Hu, W., and Wang, Z.L. (2016a). Freestanding flag-type triboelectric nanogenerator for harvesting high-altitude wind energy from arbitrary directions. ACS Nano *10*, 1780–1787.

Zhao, Z., Yan, C., Liu, Z., Fu, X., Peng, L.-M., Hu, Y., and Zheng, Z. (2016b). Machine-washable textile triboelectric nanogenerators for effective human respiratory monitoring through loom weaving of metallic yarns. Adv. Mater. *28*, 10267–10274.

Zhao, Z., Huang, Q., Yan, C., Liu, Y., Zeng, X., Wei, X., Hu, Y., and Zheng, Z. (2020). Machine-washable and breathable pressure sensors based on triboelectric nanogenerators enabled by textile technologies. Nano Energy, 104528.

Zhou, J., Wang, Z.L., Hu, Q., Zhong, Q., Zhong, J., Zhang, Y., and Hu, B. (2014a). Fiber-based generator for wearable electronics and mobile medication. ACS Nano *8*, 6273–6280.

Zhou, T., Zhang, C., Han, C.B., Fan, F.R., Tang, W., and Wang, Z.L. (2014b). Woven structured triboelectric nanogenerator for wearable devices. ACS Appl. Mater. Interfaces *6*, 14695–14701.

Zhou, K., Zhao, Y., Sun, X., Yuan, Z., Zheng, G., Dai, K., Mi, L., Pan, C., Liu, C., and Shen, C. (2020). Ultra-stretchable triboelectric nanogenerator as high-sensitive and self-powered electronic skins for energy harvesting and tactile sensing. Nano Energy *70*, 104546.

Zhu, G., Pan, C., Guo, W., Chen, C.-Y., Zhou, Y., Yu, R., and Wang, Z.L. (2012). Triboelectric-Generator-driven pulse electrodeposition for micropatterning. Nano Lett. *12*, 4960–4965.

Zhu, C., Richardson, R.M., Potter, K.D., Koutsomitopoulou, A.F., Van Duijneveldt, J.S., Vincent, S.R., Wanasekara, N.D., Eichhorn, S.J., and Rahatekar, S.S. (2016a). High modulus regenerated cellulose fibers spun from a low molecular weight microcrystalline cellulose solution. ACS Sustain. Chem. Eng. *4*, 4545–4553.

Zhu, M., Huang, Y., Ng, W.S., Liu, J., Wang, Z., Wang, Z., Hu, H., and Zhi, C. (2016b). 3D spacer fabric based multifunctional triboelectric nanogenerator with great feasibility for mechanized large-scale production. Nano Energy *27*, 439–446.

Zou, H., Zhang, Y., Guo, L., Wang, P., He, X., Dai, G., Zheng, H., Chen, C., Wang, A.C., Xu, C., and Wang, Z.L. (2019). Quantifying the triboelectric series. Nat. Commun. *10*, 1–9.

Shi, M., Zhang, J., Han, M., Song, Y., Su, Z., and Zhang, H. (2016). A single-electrode wearable triboelectric nanogenerator based on conductive & stretchable fabric. In 2016 IEEE 29th International Conference on Micro Electro Mechanical Systems, pp. 1228–1231.

**iScience, Volume *23***

## Supplemental Information

# Towards Truly Wearable Systems: Optimizing and Scaling Up Wearable Triboelectric Nanogenerators

**K.R. Sanjaya D. Gunawardhana, Nandula D. Wanasekara, and R.D. Ishara G. Dharmasena**

Supplemental note 1: Comparison of performance characteristics between common fabrics

| Property | Woven | Knitted |
|---|---|---|
| Design | two sets of yarns interlaced in right angles | single set of yarns interlooped |
| Compression | better compression | moderate compression especially before washing |
| Air permeability | moderate | high |
| Stretch and recovery | relatively low | high stretch compared to woven |
| Dimensional stability | moderate to high due to compact structure | low to moderate due to lose loop structure |
| Friction and tactile properties | correlation between friction and touch properties are lower | correlation between friction and touch properties are higher |
| Drapability | less drape | medium to high drape |
| Crease recovery | low | moderate to high |

*Table S1:Comparison of wearable properties between woven and knitted fabrics (adopted from ref* (Adanur, 2000; Spencer, 2001; Bertaux, Lewandowski and Derler, 2007; Maqsood *et al.*, 2017)*)*

Supplemental note 2: Categorization of dyes recommended for different fibre types

| Dye type | Fibre type |
|---|---|
| Acid dyes | Wool, Nylon, Silk fibres |
| Reactive dyes, Direct dyes, Vat dyes, Sulphur dyes, Azoic dyes | Cellulose fibres (cotton, viscose) |
| Disperse dyes | Polyester fibres, polypropylene fibres, and, most synthetic fibres |
| Basic dyes | Acrylic fibres |

*Table S2:Summary of different dye types and corresponding fibre types (adopted from ref* (Wardman, 2017)*)*

Supplemental Note 3: Wearable TENG developments based on common textile polymers

| Year | Triboelectric surfaces | Open circuit voltage | Short circuit current / current density | Peak power / (corresponding external load) | Remarks |
|---|---|---|---|---|---|
| 2014 (Zheng *et al.*, 2014) | Nylon, PVDF | 1163 V | 11.5 $\mu Acm^{-2}$ | 26.6 $Wm^{-2}$ (9 MΩ) | Developed with electrospun nanowires |
| 2016 (Zhang *et al.*, 2016) | Nylon, cotton | 1.5 V | 0.3 $\mu Acm^{-2}$ | - | Woven textiles sewn into conductive fabric |
| | Nylon, functionalized cotton | 8 V | 1 $\mu Acm^{-2}$ | 13 $\mu W/cm^2$ (50 MΩ) | Cotton treated with trichlorosilane |
| 2016 (Zhu *et al.*, 2016) | Nylon, PTFE | 3 V | 0.3 $\mu Acm^{-2}$ | 16 μW (0.6 MΩ) | 3D knitted spacer fabric |
| 2016 (Liu *et al.*, 2016) | PET, PDMS | 500 V | 20 μA | 153.8 $mW/m^2$ (1 GΩ) | 3D knitted spacer fabric |
| 2018 (Guo *et al.*, 2018) | Silk, PVDF | ~500 V | ~12 μA, | 310 $\mu W/cm^2$ (100 MΩ) | Piezoelectric and triboelectric hybrid structure, with silk and PVDF electrospun nanofibers |
| 2019 (Liu *et al.*, 2019) | Nylon, polyester | 6.35 V | 575 nA | 2.33 $mW/m^2$ (50 MΩ) | Core-shell yarn structure, assembled into a woven fabric |
| 2019 (Paosangthong *et al.*, 2019) | Nylon, PVC heat transfer vinyl | RMS-136 V | 2.68 μA RMS current | 38.8 $mW/cm^2$ RMS power (50 MΩ) | Grated fabric structure |
| 2019 (Jeong *et al.*, 2019) | Cotton, PDMS | 12.47 V | - | - | Twill structured woven fabrics |
| 2019 (Chang *et al.*, 2019) | Nylon, polyester | 30.96 V | 3.07 μA | 13.97 μW (10 MΩ) | Nylon layer - embroidered square array pattern, Polyester layer - consists of PVDF nanofibers |
| 2020 (Ye *et al.*, 2020) | Silk, PTFE | ~45 V | ~ 0.2 $mA/m^2$ | 3.5 $mW/m^2$ (50 MΩ) | Core-shell fibre structure, assembled into a fabric using weaving and embroidery |

*Table S3: Performance of wearable TENG developments using common textile polymers*

## Supplemental note 4: Critical yarn parameters related to common fabric manufacturing processes

During the process of fabric manufacture, yarns are sent through different yarn guides and machine elements (for example, heddle eye during weaving, and yarn feeders in knitting). Most of these guides and feeders contain mechanisms to accommodate a range of yarn diameters. The yarn diameter (*d*) is theoretical approximated using,

$$d = 2\sqrt{\frac{T}{\pi\rho}} \quad \text{(S1)}$$

where T= tex count (weight in grams per 1000 m of yarn), and, ρ= density, of the yarn.

Yarns are subjected to high stresses during fabric formation; therefore, yarn strength is also a key parameter. Textile machines can handle a range of such compatible diameters, weights and strengths. Hence, it is important that the triboelectric yarns are fibres are fabricated within these specifications to ensure their compatibility with the existing textile processes, enabling smooth scaling up. Following is a summary of most common yarn parameters used in the textile manufacturing industry, corresponding to different fabric manufacturing methods.

### S 4.1 Yarn parameters for weaving

| Weaving machine type | Weft yarn count range | Weft density range | Warp density range |
|---|---|---|---|
| Air Jet weaving | Staple spun: 6 -110 tex<br>Filament: 4.5 - 500 tex | 3.5 – 140 per cm | 3 -111 per cm |
| Projectile (p-lean weaving) | Staple spun 15 - 60 tex | 10 - 40 per cm | 10 - 40 per cm |
| Rapier weaving | 5 -1000 tex | 2—250 per cm | Varies according to warp yarn count |

*Table S4: Weft yarn count, weft density and warp density details for different weaving processes. Adopted from ref* (Adanur, 2000).

| Yarn parameter | Up to 15 tex | Above 15 tex |
|---|---|---|
| Single yarn tenacity* | 20 g / tex | 20 g / tex |
| Maximum percentage variation for yarn count | Up to 1.2% | Up to 1.4 % |
| Elongation at break percentage | Above 5.5% | Above 6% |

*Table S5: Yarn specifications required for high speed weaving. Adopted from ref* (Saket Projects Limited, 2013).

*tenacity is a measure of strength of a yarn, calculated as a ratio between the ultimate breaking strength of the yarn and its linear density (in tex).

S4.2 Yarn parameters for knitting

| Machine gauge** | Single jersey | rib | Interlock |
|---|---|---|---|
| 8 | ~84 – 169 tex | ~49 – 62 tex | - |
| 10 | ~69 – 124 tex | ~33 – 49 tex | ~49 – 71 tex |
| 12 | ~59 – 112 tex | ~29.5 – 42 tex | ~42 – 54 tex |
| 14 | ~49 – 84 tex | ~25 – 36 tex | ~36 – 49 tex |
| 16 | ~31 – 49 tex | ~17 – 36 tex | ~27 – 36 tex |
| 18 | ~25 – 42 tex | ~12 – 20 tex | ~25 – 27 tex |
| 20 | ~23 – 33 tex | ~11 – 14 tex | ~20 – 25 tex |
| 22 | ~20 – 27 tex | ~10 – 12 tex | ~17 – 20 tex |
| 24 | ~17 – 25 tex | ~8 – 11 tex | ~14 – 18 tex |
| 26 | ~14 – 23 tex | - | ~12 – 17 tex |
| 28 | ~12 – 20 tex | - | ~11 – 14 tex |
| 30 | ~10 – 17 tex | - | ~10 – 12 tex |

*Table S6: Yarn counts specified for single jersey, rib and interlock structures against different knitting gauges, commonly used in the industry. Adopted from ref.* (Kothari, 2013).

**The machine gauge indicates the number of needles per inch in a knitting machine.

Supplemental note 5: Summary of sewing thread parameters

| Parameter | Measurement method | Expected result |
|---|---|---|
| Thread twist (number of twists per yarn unit length) | Using test standards ASTM D1423 for plied thread, and, ASTM D1422 for single threads | Average twist[+] |
| Twist direction | Empirical testing and visual inspection (S direction and Z direction twists are available) | Twist direction appropriate for the sewing machine type (Z - single needle lock stitch, double needle lock stitch; S - two needle lock stitch) |
| Twist balance | Tested using standard ASTM D204 | Balanced twist[++] |
| Strength | Tensile strength, tenacity and elongation are measured using ASTM D2256 | Withstand frictional forces and elevated temperature during processing[+++] |
| Thread uniformity | Physical examination | Minimize thick or thin places, or, knots along the yarn |
| Thread size | Tested using thickness gauge, using ASTM D204 standard | Compatible with needle eye size |
| Shrinkage | ASTM D204 | Low shrinkage |

*Table S7: Sewing thread parameters, measurement methods, and expected outcomes. Adopted from ref* (Ahmad *et al.*, 2017).

+ If the twist is too high, there will be loops forming on the thread which prohibits stitch formation, whereas, too low twist causes low strength.

++ Balanced twist stops snarling /kinking (tendency of yarn twist or curl by bending upon itself).

+++ Frictional forces will be exerted by thread guides, take-up levers, tension disks, and the needle eye during subsequent processing. Threads should also be able to withstand the elevated temperature at the needle point.

Supplemental note 6: Some of the significant textile based TENG developments, listed based on the fabric type

| Year | Fabric type | Triboelectric Surfaces | Conductive surface | Electrical performance testing conditions | Max. voltage | Max. current / current density | Charge / charge density | Max. power/ (external Load resistance) |
|---|---|---|---|---|---|---|---|---|
| 2014 (Zhou *et al.*, 2014) | Woven | Nylon fabric, Polyester fabric, | Silver fabric | Linear motor acceleration- 50 m/s$^2$, max speed-1.2 m/s, amplitude-12 mm | 95 V | 2.5 μA, | 9.6 μC/m$^2$ | - |
| 2015 (Ko, Nagaraju and Yu, 2015) | Woven | PDMS, Ni | Ni coated PET | 3.5 - 4 kgf pushing force applied at a frequency of 0.5 Hz | 8.12 V | 25.77 nA/cm$^2$ | - | 0.125 μW/cm$^2$ (1 MΩ) |
| 2015 (Kim *et al.*, 2015) | Woven | PDMS, Au/Al | Au/Al, Al | Compressive force of ~50 N at frequency of 10 Hz | 40 V | 210 μA | - | 4 mW (10 MΩ) |
| 2015 (Pu *et al.*, 2015) | Woven | Parylene, Ni | Ni coated polyester | Pressing with hand | 50 V | 4 μA, | - | 393.7 mW/m$^2$ (70 MΩ) |
| 2015 (Seung *et al.*, 2015) | Woven | Ag, PDMS nanopatterned using ZnO nanorods | Ag | 10 kgf compression force | 120 V | 65 μA | - | 1.1 mW (1 MΩ) |
| 2015 (Lee *et al.*, 2015) | Woven | PDMS, Al | Al nanoparticle grown over Au, Au | Voltage and current - bending at 100 mm/s and 3 cm length<br>Power - 20 mm/s speed and 3 cm length | 368 V | 78 μA | - | 33.6 mW/cm$^2$ (20 Ω) |
| 2016 (Pu *et al.*, 2016) | Woven | Parylene, Ni | Ni | 0.75 m/s sliding speed | - | 55 μA | - | 3.2 W/m$^2$ |
| 2016 (Zhu *et al.*, 2016) | Knitted | Nylon, PTFE | Graphene | 3 Hz frequency | 3.3 V/cm$^2$ | 0.3 μA/cm$^2$ | - | ~16 μW/cm$^2$ (0.6 MΩ) |
| 2017 (Kwak *et al.*, 2017) | Knitted | PTFE, Ag | Ag | 30% strain at 1.7 Hz frequency | 23.50 V | 1.05 μA | - | 60 μW (5 MΩ) |
| 2017 (Zhao *et al.*, 2016) | Woven | PA, Cu | Cu coated PET | Tapping at 10 cm/s | 4.98 V | 15.50 mA/m$^2$ | - | 33.16 mW/m$^2$ (60 MΩ) |
| 2017 (Dong *et al.*, 2017) | Woven | PDMS, Stainless steel | Stainless steel | Voltage, current, charge -5 Hz frequency and 25 mm amplitude tapping<br>Power - 3 Hz frequency | ~45 V | $I_{SC}$~1.8 μA | ~18 nC | 263.36 mW/m$^2$ (132 MΩ) |
| 2017 (Choi *et al.*, 2017) | Knitted Woven hybrid | Silk, Silicon rubber | Ag coated nylon | Vertical pressing force of 1 kgf | 119.1 V | 26.1 μA | - | 16.6 μW/cm$^2$ (40 Ω) |

| | | | | | | | | |
|---|---|---|---|---|---|---|---|---|
| 2018 (Ning *et al.*, 2018) | Woven | PTFE, Cotton | Cu | Mechanical impact frequency of 30 Hz | 780 V | 4.9 μA | 24.1 nC | 0.56 W/$m^2$ (100 MΩ) |
| 2018 (Chen *et al.*, 2018) | Woven | Cotton, PTFE | Carbon | 20 cm/s sliding speed | ~118 V | ~1.5 μA | 48 nC | - |
| 2018 (Li *et al.*, 2018) | Knitted | Nylon 6, PTFE | Ag | Not specified | 80 V | 4 μA | - | 11.0 mW/ $m^2$ (10 MΩ) |
| 2018 (Xiong *et al.*, 2018) | Woven | Black phosphorous encapsulated HCOENP, skin | Ag | 5 N force at 6 Hz frequency | 880 V | 1.1 μA/$cm^2$ | - | 0.52 mW/$cm^2$ (100 MΩ) |
| 2019 (Liu *et al.*, 2019) | Woven | Nylon, polyester | Cu, Steel | Sliding displacement of 8 mm and 0.15 m/s | 6.35 V | 575 nA | - | 2.33 mW/$m^2$ (50 MΩ) |
| 2019 (Chen *et al.*, 2019) | Knitted | PET, Silicone | Ag | Voltage, current, charge - stretching at 4 Hz frequency<br>Power- applying a pressure of 0.4kPa | 1.2 V | 6.04 nA | 0.4 nC | 3.4 mW/$m^2$ (200 MΩ) |
| 2020 (Chen *et al.*, 2020) | Woven | Nylon, PTFE, Ag | Ag | 0.01 m/s for a moving distance of 20 mm, with a weight of 1 kg | 4500 V (DC) | 40 μA (DC) | 4.47 μC | - |

*Table S8: A summary of power output, open circuit voltage, and short circuit current for several fabric based TENG examples.*

Supplemental note 7: Processability requirements and wearable considerations for fabric related TENG

## S7.1 Fabric weight categories and related applications

| Weight category | properties | Related products |
|---|---|---|
| very lightweight (<1 ounce per square yard (oz $Yrd^2$)) | Highly breathable, wrinkles well, high opacity | Broadcloths, linen blend fabrics, some cotton fabrics |
| Light weight (2 – 3 oz $yrd^2$) | Wrinkles well, less creasing | Curtain materials, slipcover for furniture, lingerie, business wear |
| Medium weight (5 – 7 oz $yrd^2$) | Low opacity, less wrinkling | General clothing including T Shirts, Shirts etc. |
| Heavy weight (>7 oz $yrd^2$) | Good insulation, high tearing strength | Technical textiles, upholstery, denims, safety products |

*Table S9: common properties and related products for different fabric weight categories* (Li and Dai, 2006; Fairhurst, 2008; Montano and Sommerstein, 2011).

## S7.2 Fabric thermal conductivity for different applications

| Clothing type | Clo value* | Clothing type | Clo value |
|---|---|---|---|
| T shirt | 0.09 | Light trousers | 0.26 |
| Long underwear | 0.1 | Heavy trousers | 0.32 |
| Light shirt long sleeve | 0.22 | Heavy jacket | 0.49 |
| Heavy shirt long sleeve | 0.29 | Socks knee high | 0.1 |
| Light dress women | 0.22 | Heavy slacks women | 0.44 |
| Heavy dress women | 0.70 | Bra and panties | 0.05 |

*Table S10: Clo values specified for different clothing types adopted from ref* (Bartels, 2011)

*clo value - the amount of clothes required by an inactive person to be comfortable at a room temperature of 21 °C. (1 clo = 0.155 $m^2$ °C/W).

Supplemental note 8: Some of the main wearable consideration and corresponding test standards for textiles

| Test Category | Specimen | Textile Property | Test standard |
|---|---|---|---|
| Structural testing | Fibre/yarn | linear density of (weight) | ASTM D1577 - 07(2018) |
| | | Evenness | ASTM D1425 / D1425M - 14(2020) |
| | Fabric | Area density | ASTM D3776 / D3776M - 09a (2017)<br>ISO 3801:1977 |
| | | Thickness | ASTM D1777 - 96(2019) |
| | | Drapability | Pierce's cantilever method/ Rotrakote CISICK drape tester /3D body scanner techniques |
| Durability testing | Fibre/yarn | Tensile strength | ASTM D2256 / D2256M - 10(2015) |
| | Fabric | Tensile strength | ISO 13934-1:1999/ ASTM D5035-95/ AS 4878.6-2001(for coated fabrics) |
| | | Tearing strength (specially woven) | ISO 4674-1998 /ASTM D1423-83/ BS 3424 standard (for coated fabrics) |
| | | Bursting strength (specially knitted) | ISO 3303-1995/ BS 3424/ ASTM D3787 |
| | | Abrasion resistance | ISO 13934-1:2013/ ASTM D5035 - 11(2019) |
| | | Dimensional stability after washing | BS EN ISO 3759:1995 / BS EN ISO 6330:2001 |
| | | Electrical conductivity after laundering (for conductive textiles) | ASTM (ASTM WK61480) |
| Comfort and aesthetic related testing | Fabric | Air permeability | BS 5636<br>ASTM D 7534 |
| | | Moisture management | AATCC 195 |
| | | Thermal comfort | ASTM D7140 / D7140M - 13(2017) |
| | | Colour fastness | ISO-105 |
| Safety testing | Fabric | Flammability | BS 5438/ EN ISO 6941/ BS EN ISO 15025:2002/ BS EN 367:1992 (ISO 9151) |
| Intelligent testing | Fabric | Shape memory effect of fabric | AATCC 66-1998 |
| | | Superhydrophobic property | AATCC 195 |
| | | Electrical conductivity | BS EN IEC 63203-201-1/ BS EN IEC 63203-201-3 |

*Table S11: Test standards for textiles that are useful for wearable TENGs. Adopted from ref* (Hu, 2008; AATCC, 2011; Ruchira Nalinga Wijesena *et al*., 2016; *ASTM D7140 / D7140M - 13(2017) Standard Test Method to Measure Heat Transfer Through Textile Thermal Barrier Materials*, 2017; ASTM, 2017, 2018, 2019; Niles, 2017; Niles *et al*., 2017; Sala de Medeiros *et al*., 2019; BSI, 2019, 2020)

Supplemental note 9: Restrictions for Hazardous chemical usage

| Chemical substrate | Maximum Permitted Limits | | |
|---|---|---|---|
| Formaldehyde | 30 ppm for children's clothing (EU)<br>75 ppm for direct skin contact textiles (Japan) | | |
| **Heavy metals** | **Baby wear (ppm)** | **With skin contact (ppm)** | **No skin contact (ppm)** |
| Antimony | 30 | 30 | 30 |
| Copper | 25 | 50 | 50 |
| Nickel | 1 | 4 | 4 |
| Lead | 0.2 | 1 | 1 |
| chlorinated phenolic compounds | 1 mg/kg (EU) | | |
| Organotin compounds (Dibutyltin, tributyltin, triphenyltin ) | 0.5-1 mg/kg | | |
| Chlorine organic carriers | <1 mg/kg | | |
| Phthalates | 500 mg/kg (individual component) | | |

*Table S12: Hazardous chemical substance restrictions (adopted from ref* (Das, 2013)*).*

References


AATCC (2011) 'Liquid Moisture Management Properties of Textile Fabrics', *Test Method 195-2011*, pp. 366–370.

Adanur, S. (2000) *Handbook of Weaving*. 1st edn, *Handbook of Weaving*. 1st edn. CRC Press. doi: 10.1201/9781420031966.

Ahmad, S. *et al.* (2017) *Advanced Textile Testing Techniques*, *Advanced Textile Testing Techniques*. Edited by S. Ahmad et al. CRC Press. doi: 10.4324/9781315155623.

ASTM (2017) *WK61480 New Test Method for Durability of Smart Garment Textile Electrodes after Laundering*. Available at: https://www.astm.org/DATABASE.CART/WORKITEMS/WK61480.htm (Accessed: 23 February 2020).

ASTM (2018) *Subcommittee D13.50 : Published standards under D13.50 jurisdiction*. Available at: https://www.astm.org/COMMIT/SUBCOMMIT/D1350.htm (Accessed: 15 May 2020).

ASTM (2019) 'ASTM International - BOS Volume 06.01'. Available at: https://www.astm.org/BOOKSTORE/BOS/TOCS_2019/07.01.html (Accessed: 15 May 2020).

*ASTM D7140 / D7140M - 13(2017) Standard Test Method to Measure Heat Transfer Through Textile Thermal Barrier Materials* (2017). Available at: https://www.astm.org/Standards/D7140.htm (Accessed: 23 February 2020).

Bartels, V. T. (2011) 'Improving comfort in sports and leisure wear', in *Improving Comfort in Clothing*. Elsevier Ltd., pp. 385–411. doi: 10.1016/B978-1-84569-539-2.50015-6.

Bertaux, E., Lewandowski, M. and Derler, S. (2007) 'Relationship between Friction and Tactile Properties for Woven and Knitted Fabrics', *Textile Research Journal*, 77(6), pp. 387–396. doi: 10.1177/0040517507074165.

BSI (2019) *19/30394009 DC - BS EN IEC 63203-201-3. Wearable electronic devices and technologies. Part 201-3. Electronic Textile. Determination of electrical resistance of conductive textiles under simulated microclimate*. Available at: https://shop.bsigroup.com/ProductDetail?pid=000000000030394009 (Accessed: 15 May 2020).

BSI (2020) *20/30387889 DC - BS EN IEC 63203-201-1. Wearable electronic devices and technologies. Part 201-1. Electronic Textile. Measurement methods for basic properties of conductive yarns*. Available at: https://shop.bsigroup.com/ProductDetail?pid=000000000030387889 (Accessed: 15 May 2020).

Chang, C. C. *et al.* (2019) 'Development of textile-based triboelectric nanogenerators integrated with plastic metal electrodes for wearable devices', *International Journal of Advanced Manufacturing Technology*. The International Journal of Advanced Manufacturing Technology, 104(5–8), pp. 2633–2644. doi: 10.1007/s00170-019-04160-9.

Chen, C. *et al.* (2019) '3D double-faced interlock fabric triboelectric nanogenerator for bio-motion energy harvesting and as self-powered stretching and 3D tactile sensors', *Materials Today*. Elsevier Ltd, xxx(xx), pp. 1–10. doi: 10.1016/j.mattod.2019.10.025.

Chen, C. *et al.* (2020) 'Direct Current Fabric Triboelectric Nanogenerator for Biomotion Energy Harvesting', *ACS Nano*, 14(4), pp. 4585–4594. doi: 10.1021/acsnano.0c00138.

Chen, J. *et al.* (2018) 'Traditional weaving craft for one-piece self-charging power textile for wearable electronics', *Nano Energy*, 50, pp. 536–543. doi: 10.1016/j.nanoen.2018.06.009.

Choi, A. Y. *et al.* (2017) 'Corrugated Textile based Triboelectric Generator for Wearable Energy Harvesting', *Scientific Reports*. Nature Publishing Group, 7, pp. 7–12. doi: 10.1038/srep45583.

Das, S. (2013) *Product Safety and Restricted Substances in Apparel*. 2nd edn, *Product Safety and Restricted Substances in Apparel*. 2nd edn. WPI Publishing. doi: 10.1201/b18884.

Dong, K. *et al.* (2017) '3D Orthogonal Woven Triboelectric Nanogenerator for Effective Biomechanical Energy Harvesting and as Self-Powered Active Motion Sensors', *Advanced Materials*, 29(38), pp. 1–11. doi: 10.1002/adma.201702648.

Fairhurst, C. (2008) *Advances in apparel production*, *Advances in Apparel Production*. Woodhead Pub. in association with the Textile Institute. doi: 10.1533/9781845694463.

Guo, Y. *et al.* (2018) 'All-fiber hybrid piezoelectric-enhanced triboelectric nanogenerator for wearable gesture monitoring', *Nano Energy*. Elsevier Ltd, 48, pp. 152–160. doi: 10.1016/j.nanoen.2018.03.033.

Hu, J. (2008) *Fabric testing*, *Fabric Testing*. Woodhead Publishing Limited. doi: 10.1533/9781845695064.

Jeong, J. *et al.* (2019) 'Comparative Study of Triboelectric Nanogenerators with Differently Woven Cotton Textiles for Wearable Electronics', *Polymers*, 11(9), p. 1443. doi: 10.3390/polym11091443.

Kim, K. N. *et al.* (2015) 'Highly Stretchable 2D Fabrics for Wearable Triboelectric Nanogenerator under Harsh Environments', *ACS Nano*, 9(6), pp. 6394–6400. doi: 10.1021/acsnano.5b02010.

Ko, Y. H., Nagaraju, G. and Yu, J. S. (2015) 'Multi-stacked PDMS-based triboelectric generators with conductive textile for efficient energy harvesting', *RSC Advances*. Royal Society of Chemistry, 5(9), pp. 6437–6442. doi: 10.1039/C4RA15310C.

Kothari, V. (2013) '19 Yarn Requirement for Knitting', (February 2013), pp. 28–30. Available at: https://www.academia.edu/12875039/19_Yarn_Requirement_for_Knitting (Accessed: 14 May 2020).

Kwak, S. S. *et al.* (2017) 'Fully Stretchable Textile Triboelectric Nanogenerator with Knitted Fabric Structures', *ACS Nano*, 11(11), pp. 10733–10741. doi: 10.1021/acsnano.7b05203.

Lee, S. *et al.* (2015) 'Triboelectric energy harvester based on wearable textile platforms employing various surface morphologies', *Nano Energy*. Elsevier, 12, pp. 410–418. doi: 10.1016/j.nanoen.2015.01.009.

Li, H. *et al.* (2018) 'A Compound Yarn Based Wearable Triboelectric Nanogenerator for Self-Powered Wearable Electronics', *Advanced Materials Technologies*, 3(6), p. 1800065. doi: 10.1002/admt.201800065.

Li, Y. and Dai, X. Q. (2006) *Clothing comfort and compression therapy*, *Biomechanical Engineering of Textiles and Clothing*. doi: 10.1533/9781845691486.2.145.

Liu, J. *et al.* (2019) 'Core-Shell Fiber-Based 2D Woven Triboelectric Nanogenerator for Effective Motion Energy Harvesting', *Nanoscale Research Letters*, 14(1), p. 311. doi: 10.1186/s11671-019-3144-2.

Liu, L. *et al.* (2016) 'A triboelectric textile templated by a three-dimensionally penetrated fabric', *Journal of Materials Chemistry A*, 4(16), pp. 6077–6083. doi: 10.1039/C6TA01166G.

Maqsood, M. *et al.* (2017) 'Comparison of compression properties of stretchable knitted fabrics and bi-stretch woven fabrics for compression garments', *Journal of the Textile Institute*, 108(4), pp. 522–527. doi: 10.1080/00405000.2016.1172432.

Montano, M. and Sommerstein, C. (2011) *Window Treatments and Slipcovers For Dummies*. John Wiley & Sons.

Niles, S. (2017) 'A Vision-Based Method for the Assessment of Colour Fastness to Washing', *International Journal for Research in Applied Science and Engineering Technology*, V(II), pp. 550–556. doi: 10.22214/ijraset.2017.2081.

Niles, S. N. *et al.* (2017) 'A Vision-Based Method For Analyzing Yarn Evenness', *International Journal of Scientific & Technology Research*, 6(2), pp. 254–256.

Ning, C. *et al.* (2018) 'Washable textile-structured single-electrode triboelectric nanogenerator for self-powered wearable electronics', *Journal of Materials Chemistry A*, 6(39), pp. 19143–19150. doi: 10.1039/c8ta07784c.

Paosangthong, W. *et al.* (2019) 'Textile-based triboelectric nanogenerator with alternating positive and negative freestanding grating structure', *Nano Energy*. Elsevier Ltd, 66, p. 104148. doi: 10.1016/j.nanoen.2019.104148.

Pu, X. *et al.* (2015) 'A self-charging power unit by integration of a textile triboelectric nanogenerator and a flexible lithium-ion battery for wearable electronics', *Advanced Materials*, 27(15), pp. 2472–2478. doi: 10.1002/adma.201500311.

Pu, X. *et al.* (2016) 'Wearable Power-Textiles by Integrating Fabric Triboelectric Nanogenerators and Fiber-Shaped Dye-Sensitized Solar Cells', *Advanced Energy Materials*, 6(20), p. 1601048. doi: 10.1002/aenm.201601048.

Ruchira Nalinga Wijesena *et al.* (2016) 'NEAR INFRARED ENERGY ABSORBING TEXTILE'. Sri Lanka. Available at: https://patents.google.com/patent/US20170314185A1/en.

Saket Projects Limited, A. (2013) *Yarn Quality Requirement for Weaving | Requirements of Yarn Quality for Hide Speed Weaving - Fibre2Fashion*. Available at: https://www.fibre2fashion.com/industry-article/6810/yarn-quality-requirement-for-high-speed-weaving-machines (Accessed: 14 May 2020).

Sala de Medeiros, M. *et al.* (2019) 'Waterproof, Breathable, and Antibacterial Self-Powered e-Textiles Based on Omniphobic Triboelectric Nanogenerators', *Advanced Functional Materials*, 29(42), p. 1904350. doi: 10.1002/adfm.201904350.

Seung, W. *et al.* (2015) 'Nanopatterned textile-based wearable triboelectric nanogenerator', *ACS Nano*, 9(4), pp. 3501–3509. doi: 10.1021/nn507221f.

Spencer, D. J. (2001) *Knitting technology : a comprehensive handbook and practical guide*. 1st edn. CRC Press.

Wardman, R. H. (2017) *An Introduction to Textile Coloration*, *An Introduction to Textile Coloration*. Chichester, UK: John Wiley & Sons, Ltd. doi: 10.1002/9781119121619.

Xiong, J. *et al.* (2018) 'Skin-touch-actuated textile-based triboelectric nanogenerator with black phosphorus for durable biomechanical energy harvesting', *Nature Communications*. Springer US,

9(1), pp. 1–9. doi: 10.1038/s41467-018-06759-0.

Ye, C. *et al.* (2020) 'Ultrastable and High-Performance Silk Energy Harvesting Textiles', *Nano-Micro Letters*. Springer Singapore, 12(1), pp. 1–15. doi: 10.1007/s40820-019-0348-z.

Zhang, L. *et al.* (2016) 'All-Textile Triboelectric Generator Compatible with Traditional Textile Process', *Advanced Materials Technologies*, 1(9), p. 1600147. doi: 10.1002/admt.201600147.

Zhao, Z. *et al.* (2016) 'Machine-Washable Textile Triboelectric Nanogenerators for Effective Human Respiratory Monitoring through Loom Weaving of Metallic Yarns', *Advanced Materials*, 28(46), pp. 10267–10274. doi: 10.1002/adma.201670325.

Zheng, Y. *et al.* (2014) 'An electrospun nanowire-based triboelectric nanogenerator and its application in a fully self-powered UV detector', *Nanoscale*, 6(14), pp. 7842–7846. doi: 10.1039/c4nr01934b.

Zhou, T. *et al.* (2014) 'Woven Structured Triboelectric Nanogenerator for Wearable Devices', *ACS Applied Materials & Interfaces*, 6(16), pp. 14695–14701. doi: 10.1021/am504110u.

Zhu, M. *et al.* (2016) '3D spacer fabric based multifunctional triboelectric nanogenerator with great feasibility for mechanized large-scale production', *Nano Energy*. Elsevier, 27, pp. 439–446. doi: 10.1016/j.nanoen.2016.07.016.